Chapter 2
Modeling of LPV Systems

Introduction

In general terms, control theory can be described as the study of how to design the process of influencing the behavior of a physical system to achieve a desired goal. An open-loop control is one in which the control input is not affected in any way by the actual (measured) outputs. If the system changes during the operational time then the control performance can be severely reduced. In a closed-loop system the control input is affected by the measured outputs, i.e., a feedback is being applied to that system. Very often a reference input is given, which is directly related to the desired value of system outputs, and the purpose of the controller will be to minimize the error between the actual system output and the desired (reference input) value.

There are two main features in the analysis of a control system: system modeling, which means expressing the physical system under examination in terms of a model (or models) which can be readily dealt with and understood, and the design stage, in which a suitable control strategy is both selected and implemented in order to achieve a desired system performance. Forming a mathematical model which represents the characteristics of a physical system is crucially important as far as the further analysis of that system is concerned.

Traditionally controllability and observability are the main issues in the analysis of a system before deciding the best control strategy to be applied, or whether it is possible to control or stabilize the system. Controllability is related to the possibility of forcing the system into a particular state by applying an appropriate control signal while observability is related to the possibility of reconstructing, through output measurements, the state of a system.

The model should not be over simple so that important properties of the system are not included, something that would lead to an incorrect analysis or an inadequate controller design. In some cases the nonlinear characteristics are so important that they must be dealt with directly, and this can be quite a complex procedure.

© Springer International Publishing Switzerland 2017

P. Gáspár et al., *Robust Control Design for Active Driver Assistance Systems*,
Advances in Industrial Control, DOI 10.1007/978-3-319-46126-7_2

Gain-scheduling is a technique widely used to control such systems in a variety of engineering applications. In the classical gain scheduling approach, having strong roots in flight control applications, the controller synthesis is based on local descriptions of the nonlinear system, that can most often be approximated by linear system properties. The gains of the gain-scheduled controllers are typically chosen using linear control design techniques and is a two step process. First, several operating points are selected to cover the range of system dynamics. At each of these points, the designer makes an LTI approximation to the plant and then, designs a linear compensator for each linearized plant. This process gives a set of linear feedback control laws that perform satisfactorily when the closed-loop system is operated near the respective operating points. A global nonlinear controller for the nonlinear system is then obtained by interpolating, or scheduling, the gains from the local operating point designs.

Since the synthesized controllers are guaranteed to satisfy specifications only locally, the designer typically cannot assess a priori the stability, robustness, and performance properties of gain-scheduled controller designs. While the local controller synthesis can be performed using the well established techniques of the linear system theory, it remains a non-trivial procedure to map the linear controllers such that non-local specifications of the closed loop system are kept.

The LPV paradigm provides a remedy to this problem, Shamma and Athans (1990), Shamma (1992). Initiated in Shamma and Athans (1991) LPV modeling techniques have gained a lot of interest, especially those related to vehicle and aerospace control, Becker and Packard (1994), Balas et al. (1997), Marcos and Balas (2001), Szászi et al. (2005). LPV systems have recently become popular as they provide a systematic means of computing gain-scheduled controllers. In this framework the system dynamics are written as a linear state-space model with the coefficient matrices functions of external scheduling variables. Assuming that these scheduling variables remain in some given range then analytical results can guarantee the level of closed loop performance and robustness. The parameters are not uncertain and can often be measured in real-time during system operation. However, it is generally assumed that the parameters vary slowly in comparison to the dynamics of the system. LPV based gain-scheduling approaches are replacing ad-hoc techniques and are becoming widely used in control design.

Many of the control system design techniques using LPV models can be cast or recast as convex problems that involve LMIs. Significant progress has been made recently in the use of LMI and $\mathscr{H}_\infty$ optimization in gain-scheduled control. One such control design technique, described by Apkarian et al. (1995), is the Lyapunov function/quadratic $\mathscr{H}_\infty$ approach wherein a single Lyapunov function is sought to bound the performance of the LPV system. Such a framework generally has a strong form of robust stability with respect to time-varying parameters. However, due to the continuous variation of scheduling parameters,such a synthesis approach is generally associated with a convex feasibility problem with infinite constraints imposed on the LMI formulation. This problem can be addressed by using affine LPV modeling that reduces the infinite constraints imposed on the LMI formation to a finite number.

Such a modeling approach has been used to solve design problems by Becker (1992), Sun and Postlethwaite (1998).

The above pure LPV model is not quite matched to the control problems where the scheduling variables are in fact system states (e.g., vehicle speed), rather than bounded external variables. An approach to this problem is to generate so-called quasi-LPV models, which are applicable when the scheduling variables are measured states, the dynamics are linear in the inputs and other states, and there exist inputs to regulate the scheduling variables to arbitrary equilibrium values.

These methods concentrate on robust performance, hence, robust stability of the controlled system. In this more general context such robust control problems—both analysis and synthesis—can be formulated using a generalized plant technique based on an LFT description of the uncertain LPV system, see, e.g., Iwasaki and Hara (1998), Iwasaki and Shibata (2001), Wu (2001). The controller synthesis leads to bilinear matrix inequalities (BMI) but often it is possible to reduce the problem to the solution of a finite set of LMIs, for details see, e.g., Scherer et al. (1997), Scherer (2001), Wu (2001).

2.1 LPV Model Structures

The mathematical model of a dynamic evolution of a nonlinear, non-autonomous physical system is usually formulated as a state space representation in terms of the input $u(t) \in \mathbb{R}^m$, output $y(t) \in \mathbb{R}^p$ and state signals $x(t) \in \mathbb{R}^n$ related by a first-order differential equation:

$$\dot{x} = f(x, u, w), \tag{2.1}$$

$$y = h(x, u, w), \tag{2.2}$$

subject to the initial condition $x(t_0) = x_0$. Usually the model also describes the effect of the outer disturbances, which are modeled through the signal $w(t) \in \mathbb{R}^d$. In what follows for the sake of simplicity we concentrate on the undisturbed system, i.e., w will be suppressed from the model.

According to the LPV paradigm, parameter-dependent systems are linear systems, whose state-space descriptions are known functions of time-varying parameters. While the time variation of each of the parameters is not known in advance, it is assumed to be measurable in real time. Thus, in the LPV controller synthesis step the parameters are regarded as freely varying parameters taking arbitrary values in the region Ω and, hence, the LPV description will differ from the nonlinear system. The larger this difference, the more conservatism is introduced in the LPV controller synthesis step. LPV descriptions of nonlinear systems are not unique: it is desirable to have an LPV description that in some sense is close to the nonlinear system for all parameter values.

Thus, the aim of the LPV modeling procedure is to find an LPV description of the nonlinear model on the form

$$\dot{x} = A(\rho)x + B(\rho)u \simeq f(x,u), \quad \rho \in \Omega \tag{2.3}$$
$$y = C(\rho)x + D(\rho)u \simeq h(x,u), \tag{2.4}$$

where ρ is the, possibly state dependent, parameter vector varying within a region Ω, such that the known relation $\rho = \sigma(y,r)$ depends only on the measured signals y and exogenous signals r whose values are known in operational time.

This guarantees that the parameter values are available to the controller and that an explicit nonlinear feedback controller can be obtained from the designed LPV controller. In order to ensure that trajectories of the original nonlinear system are equal or at least closed to the trajectories of the LPV description, (2.3) should be as close to the nonlinear system as possible for all parameter values in the region Ω.

Hence, an LPV model is defined as a linear model whose state-space matrices depend on a vector ρ of time-varying parameters of the form

$$\dot{x} = A(\rho)x + B(\rho)u, \tag{2.5}$$
$$y = C(\rho)x + D(\rho)u, \tag{2.6}$$

where it is often suppose that the parameter dependency has an explicit structure: namely either affine, polynomial, polytopic or an LFT dependency. Accordingly, if

$$S(\rho) = \sum_{i=0}^{n} \sum_{|\underline{j}|=i} \rho^{\underline{j}} S_{i,\underline{j}}, \tag{2.7}$$

where $\rho^{\underline{j}} = \rho_1^{j_1}\rho_2^{j_2}\cdots\rho_k^{j_k}$ with ρ_l are the components of the parameter vector ρ, $|\underline{j}| = \sum_{l=1}^{k} i_k$ and

$$S \sim \begin{pmatrix} A & B \\ C & D \end{pmatrix}, \quad S_{i,\underline{j}} \sim \begin{pmatrix} A_{i,\underline{j}} & B_{i,\underline{j}} \\ C_{i,\underline{j}} & D_{i,\underline{j}} \end{pmatrix},$$

then $n = 1$ corresponds to the affine models. Affine models are mostly involved in applications where geometric techniques are to be used.

For polytopic LPV models the system matrix $S(\rho)$ varies within a fixed polytope of matrices: it is a convex combination $S(\rho) \in \text{convex}\{ S_1, S_2, \ldots, S_k \}$ of the system matrices (vertex systems), i.e.,

$$S(\rho) = \sum_{i=1}^{k} \rho_i S_i, \quad \rho_i \geq 0, \quad \sum_{i=1}^{k} \rho_i = 1. \tag{2.8}$$

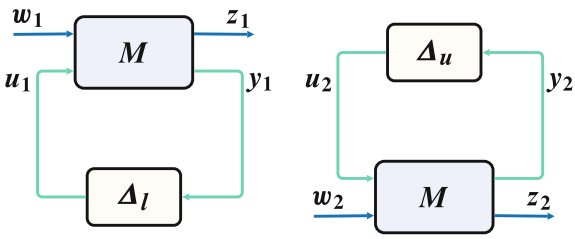


Fig. 2.1 Lower and upper LFT representations

Since polytopic models are well suited for Lyapunov-based analysis and design, they are very popular model candidates in the LPV framework.

A more general representation is the LFT, see Fig. 2.1. LFT is a representation of a system using a feedback interconnection between two operators, a known causal system

$$M = \begin{pmatrix} M_{11} & M_{12} \\ M_{21} & M_{22} \end{pmatrix}$$

and a causal bounded system Δ of proper dimension:

$$\mathcal{F}_L(M, \Delta) = M_{11} + M_{12}\Delta(I - \Delta M_{22})^{-1}M_{21} \tag{2.9}$$

$$\mathcal{F}_U(M, \Delta) = M_{22} + M_{21}\Delta(I - \Delta M_{11})^{-1}M_{12} \tag{2.10}$$

Δ is typically norm-bounded, $||\Delta||_\infty \leq 1$, but otherwise unrestricted in form (structured/un-structured) or type (nonlinear/time-varying/constant). If some of the components in the Δ operator are scheduling parameters an LPV system is obtained. This form is obtained by extracting a varying parameter from a system and placing it into a feedback loop, such that the remaining system, M, is time-invariant. Models with affine or polynomial parameter dependencies can be transformed exactly to a LFT. An important property of LFT systems is that their interconnection (e.g., sum, concatenation) and also the inversion, if it exists, always results in another LFT.

We emphasize that an LPV plant can be viewed either as an LTI plant subject to a time-varying parametric uncertainty $\rho(t)$, see, e.g., the LFT LPV structure or as a set of models of linear time-varying (LTV) plants, where each LTV system corresponds to a specific parameter trajectory. In the analysis and design process we chose the most convenient interpretation that fit the actual technique that we might use.

2.2 Linearization Through LPV Modeling

Practically, concerning the structure of the models, prior to the design and analysis phase there is no significant difference between LPV models and those used for gain scheduling. All of them can be obtained by using different, application specific,

methods. The direct linearization schemes applied to nonlinear systems can be roughly classified into the following types: linearization about an equilibrium, linearization about a parametrized state trajectory and global linearization. In the first case the system is represented as an LTI system locally around an equilibrium condition, while in the second approach the nonlinear system is to follow some prescribed trajectory around that it can be approximated by a family of parametrized linearizations. In the third case the original nonlinear system is approximated by a set of trajectories of a linear differential inclusion (LDI) which can represent it in the entire operation range. However, in this case there might be trajectories of the LPV model that are not actual trajectories of the original system. This might lead to a conservative analysis or design.

In what follows some of the most common techniques, e.g., classical, fuzzy and the off-equilibrium approaches, see, e.g., Leith and Leithead (2000), will be sketched.

2.2.1 Jacobian Linearization

Often in industrial settings, a finite collection of linear models is used to describe the behavior of a system throughout an operating envelope. The linearized models describe the small signal behavior of the system at a specific operating point and the collection is parametrized by one or more physical variables whose values represent this specific point. If the state variables have physical meaning, then it makes sense to develop polynomial least squares fits of the state-space matrices to get a continuous parameterization of the operating envelope.

The classical approach, using Jacobian linearization of the nonlinear model about a manifold of constant equilibria, constant operating points or set-points, is called linearization-based scheduling. When a corresponding scheduling variable ρ is chosen appropriately to parameterize the set of linear models, a parameterized family of linearized models representing the original nonlinear model results.

Considering the nonlinear plant dynamics an equilibrium or constant operating point (x_e, u_e) is defined by the equilibrium condition $f(x_e, u_e) = 0$. Assuming f is continuously differentiable at the equilibrium point, the nonlinear model is approximated by

$$\delta\dot{x} = A\delta x + B\delta u \tag{2.11}$$

$$\delta y = C\delta x + D\delta u, \tag{2.12}$$

where

$$\delta u = u - \tilde{u}, \quad \delta y = y - \tilde{y}, \quad \delta x = x - \tilde{x},$$

and

$$A = \partial_x f(x_e, u_e), \quad B = \partial_u f(x_e, u_e), \quad C = \partial_x h(x_e, u_e), \quad D = \partial_u h(x_e, u_e).$$

By considering an entire equilibrium family $(x_e, u_e) \in \Omega_e$ yields to a linear parameter-dependent linearization family $S(\rho_e)$, locally describing the nonlinear model:

$$\begin{aligned}\delta\dot{x} &= A(\rho_e)\delta x + B(\rho_e)\delta u\\ \delta y &= C(\rho_e)\delta x + D(\rho_e)\delta u.\end{aligned}$$

To obtain an LPV description for a nonlinear model, an interpolation of the stationary linearizations can be applied: e.g., by using a linear interpolation then system can be written as

$$\delta\dot{x}(t) = A(\rho)\delta x(t) \; + B(\rho)\delta u(t)$$

with

$$A(\rho) = \sum_{i=1}^{p} A_i\rho_i, \quad B(\rho) = \sum_{i=1}^{p} B_i\rho_i, C(\rho) = \sum_{i=1}^{p} C_i\rho_i, \quad D(\rho) = \sum_{i=1}^{p} D_i\rho_i, \tag{2.13}$$

where

$$\sum_{i=1}^{k} \rho_i = 1, \;\; \rho_i \geq 0, \;\; \delta x = x - x_e(\rho) \; , \delta u = u - u_e(\rho)$$

the points $(x_e^i, u_e^i) \in \Omega_e$ being stationary. The procedure, however, may give an LPV system that does not include the original nonlinear system. But if the stationary points can be chosen such that

$$\{(\partial f_x(x,u), \partial f_u(x,u))\} \subset \text{convex}\{(\partial f_x(x_e^i, u_e^i), \partial f_u(x_e^i, u_e^i))\}$$

then the LPV description (2.13) will include the nonlinear system.

A typical choice for Ω_e is to take a a specific trajectory $(\tilde{x}, \tilde{u}, \tilde{y})$, i.e., to perform the linearization of the nonlinear system (2.2) around a trajectory:

$$\begin{aligned}\delta\dot{x} &= \partial_x f(\tilde{x}, \tilde{u})\delta x + \partial_u f(\tilde{x}, \tilde{u})\delta u,\\ \delta y &= \partial_x h(\tilde{x}, \tilde{u})\delta x + \partial_u h(\tilde{x}, \tilde{u})\delta u,\end{aligned}$$

where

$$\delta u = u - \tilde{u}, \quad \delta y = y - \tilde{y}, \quad \delta x = x - \tilde{x}.$$

By taking the parameters of the specific trajectory (flight envelop) as measurable scheduling variables, the desired LPV model will be of the form

$$\dot{\xi} = A(\rho)\xi + B(\rho)\delta u$$
$$\delta y = C(\rho)\xi + D(\rho)\delta u.$$

A parameterized family of linearized models resulting from linearization-based scheduling or a number of black-box point-designs are only locally valid. In case an LPV model is based on such a set of linearized models, the accuracy of the resulting linear parameter-dependent model with respect to the original nonlinear model or plant is unknown. Classical gain scheduling is mainly restricted to local controller synthesis in stationary points. Even though nonlinear systems can be linearized along a trajectory, no gain scheduling approaches available in the literature that extends the stability region using a family of linearizations along different trajectories.

2.2.2 Off-Equilibrium Linearization

A disadvantage of classical linearization-based scheduling is the restriction to equilibrium-point modeling. Using the so-called velocity-based or off-equilibrium linearizations it is possible to enable linearization at every operating point: considering the nonlinear system

$$\dot{x} = f(x, u), \quad y = h(x, u),$$

the velocity linearization at a point (x_0, u_0) reads as

$$\dot{x} = \zeta$$
$$\dot{\zeta} = \partial f_x|_{(x_0,u_0)}\zeta + \partial f_u|_{(x_0,u_0)}\dot{u}$$
$$\dot{y} = \partial h_x|_{(x_0,u_0)}\zeta + \partial h_u|_{(x_0,u_0)}\dot{u}.$$

In this way there is a velocity-based linearization associated with every operating point of the original nonlinear system and the solutions may be pieced together. Thus, the resulting velocity-based linearization family, parameterized by ρ, globally approximates the trajectories of the nonlinear model to an arbitrary degree of accuracy. The velocity linearization is not limited to equilibrium points: as no restriction to equilibrium operating points is present, linear approximation of transient dynamics and operating points far from equilibrium operating points is also enabled.

Interpolation of linear controller based on velocity linearizations can be performed in a similar way to classical gain scheduling. However, since the velocity linearization is not an approximation in the same sense as a standard linearization scheme, it is easier to interpolate linearizations in a way such that the nonlinear system is included in the LPV description.

2.2.3 Fuzzy Linearization

One approach to gain scheduling, and thus, to LPV modeling, uses ideas from fuzzy systems, see Takagi and Sugeno (1985) to describe the nonlinear system: the plant dynamics is formulated as a blended multiple model representation such as a Takagi-Sugeno model or local model network of the form

$$\dot{x} = \sum_i f_i(x, u)\mu_i(\phi),$$
$$y = \sum_i h_i(x, u)\mu_i(\phi)$$

where the function $\phi(x, u)$ is the scheduling variable and the scalar blending weights $\mu_i \geq 0$ often are normalized to $\sum_i \mu_i = 1$.

After a linearization and blending of the individual components the typical form of the LPV model will be of the form:

$$\begin{pmatrix} \dot{x} \\ y \end{pmatrix} = S(\rho)\begin{pmatrix} x \\ u \end{pmatrix}, \tag{2.14}$$

with

$$S(\rho) = S_0 + \sum_{i \in I} \rho_i S_i, \tag{2.15}$$

where ρ_i will be the scheduling variables of the model.

2.2.4 qLPV Linearization

Quasi-LPV scheduling tries to overcome the general shortcomings of classical linearization schemes regarding local validity of the resulting model: the idea is to transform the nonlinear model to an LPV form hiding the nonlinear terms by including them in the scheduling variable. Since this process involves a transformation rather than a linearization, the resulting LPV model exactly equals the original nonlinear model.

A qLPV model may arise by considering state transformations on a class of nonlinear systems of the form:

$$\dot{x}_1 = f_1(x_1) + A_{11}(x_1)x_1 + A_{12}(x_1)x_2 + B_1(x_1)u,$$
$$\dot{x}_2 = f_2(x_1) + A_{21}(x_1)x_1 + A_{22}(x_1)x_2 + B_2(x_1)u,$$
$$y = x_1.$$

Assuming that there exist differentiable functions x_2^{eq} and u^{eq} such that for every x_1

$$0 = f_1(x_1) + A_{11}(x_1)x_1 + A_{12}(x_1)x_2^{eq} + B_1(x_1)u^{eq},$$
$$0 = f_2(x_1) + A_{21}(x_1)x_1 + A_{22}(x_1)x_2^{eq} + B_2(x_1)u^{eq}$$

is satisfied, then by applying the following state and input transformation:

$$\xi_1 = x_1, \quad \xi_2 = x_2 - x_2^{eq} \quad \nu = u - u^{eq},$$
$$\tilde{A}_{22}(\xi_1) = A_{22}(\xi_1) - \frac{dx_2^{eq}}{dx_1}|_{\xi_1} A_{12}(\xi_1) \quad \tilde{B}_2(\xi_1) = B_2(\xi_1) - \frac{dx_2^{eq}}{dx_1}|_{\xi_1} B_1(\xi_1)$$

one obtains the qLPV system

$$\dot{\xi}_1 = \tilde{A}_{12}(\xi_1)\xi_2 + \tilde{B}_1(\xi_1)\nu, \tag{2.16}$$
$$\dot{\xi}_2 = \tilde{A}_{22}(\xi_1)\xi_2 + \tilde{B}_2(\xi_1)\nu, \tag{2.17}$$
$$y = \xi_1. \tag{2.18}$$

While the system representation in (2.16)–(2.18) has a linearized appearance, it is not equivalent to a Jacobian linearization about an operating point still exactly represents the original nonlinear system. The representation is called qLPV since the exogenous parameter ξ_1 is actually a state.

If the system also depends on an exogenous parameter p, the final qLPV system will be of the form

$$\dot{\xi}_1 = \tilde{A}_{12}(\xi_1, p)\xi_2 + \tilde{B}_1(\xi_1, p)\nu, \tag{2.19}$$
$$\dot{\xi}_2 = \tilde{A}_{22}(\xi_1, p)\xi_2 + \tilde{B}_2(\xi_1, p)\nu + E_2(\xi_1, p)\dot{p}, \tag{2.20}$$
$$y = \xi_1, \tag{2.21}$$

where $E_2(\xi_1, p) = -\frac{dx_2^{eq}}{dp}|_{\xi_1}$. If no reliable measurement is available for the signal $\dot{p}$, then it can be treated as a disturbance signal which must be rejected.

In many cases it is possible to find a qLPV description of a nonlinear system more directly by hiding the nonlinearity in the parameter. As a trivial example let the nonlinear system be $\dot{x} = -\sin(x) + u$. This system can be represented by the qLPV system $\dot{x} = -\rho x$ with $\rho = \sin(x)/x$. Moreover, the resulting qLPV system exactly matches the original nonlinear system globally, provided the state x is measured. The same idea can be applied to obtain local models: e.g., take the nonlinear system $\dot{x} = -x^3 + u$, that can be described by the qLPV system $\dot{x} = -\rho x + u$, with the parameter satisfying $0 \leq \rho \leq M$. Clearly, the qLPV model become equal to the original one when $\rho = x^2$. In practice it is more likely to obtain local models, as in the combination of these cases: consider the nonlinear plant

$$\begin{aligned}\dot{x}_1 &= \sin x_1 + x_2,\\ \dot{x}_2 &= x_1^2 x_2 + u,\\ y &= x_1.\end{aligned}$$

Using $\rho_1 = \sin x_1/x_1$ and $\rho_2 = x_1^2$ the qLPV representation of the system is

$$\begin{aligned}\dot{x} &= A(\rho)x + Bu,\\ y &= Cx + Du,\end{aligned}$$

with $D = 0,\ C = \begin{pmatrix}1 & 0\end{pmatrix}$ and

$$A(\rho) = \begin{bmatrix}\rho_1 & 1\\ 0 & \rho_2\end{bmatrix} = \begin{bmatrix}0 & 1\\ 0 & 0\end{bmatrix} + \rho_1\begin{bmatrix}1 & 0\\ 0 & 0\end{bmatrix} + \rho_2\begin{bmatrix}0 & 0\\ 0 & 1\end{bmatrix},\quad B = \begin{pmatrix}0\\ 1\end{pmatrix}.$$

Concerning the vehicle dynamics models involved in this book in most of the cases first principle models of the form

$$J(\rho)\ddot{x} + b(\rho)\dot{x} + k(\rho)x = T(\rho)u \tag{2.22}$$

are available, where ρ depends only on measured signals, thus they are natural candidates to be choses as scheduling variables of a qLPV model. The advantage of these models are that they are global or they are valid at least on a domain on which the original first principle model was. A disadvantage might be the possible conservativity caused by the size of the domain Ω which ρ is supposed to belong when it turns to use the model for analysis or design.

We conclude this section by presenting a source of the LPV/qLPV models that is also of central importance concerning the topic of this book and it is related to the parameter varying choice of different weighting filters that enter in the formulation of the control problems.

2.2.5 Non-uniqueness of the LPV Models

An LPV description of a nonlinear system is not unique: as an example consider the nonlinear plant

$$\begin{aligned}\dot{x}_1 &= \sin x_1 + x_2,\\ \dot{x}_2 &= x_1 x_2 + u,\\ y &= x.\end{aligned}$$

Using $\rho_1 = \sin x_1/x_1$ and $\rho_2 = x_1$ the qLPV representation of the system is described by the system matrix

$$A(\rho) = \begin{bmatrix} \rho_1 & 1 \\ 0 & \rho_2 \end{bmatrix} = \begin{bmatrix} 0 & 1 \\ 0 & 0 \end{bmatrix} + \rho_1 \begin{bmatrix} 1 & 0 \\ 0 & 0 \end{bmatrix} + \rho_2 \begin{bmatrix} 0 & 0 \\ 0 & 1 \end{bmatrix},$$

while the choice $\rho_1 = \sin x_1/x_1$ and $\rho_2 = x_1$ leads to

$$A(\rho) = \begin{bmatrix} \rho_1 & 1 \\ \rho_2 & 0 \end{bmatrix} = \begin{bmatrix} 0 & 1 \\ 0 & 0 \end{bmatrix} + \rho_1 \begin{bmatrix} 1 & 0 \\ 0 & 0 \end{bmatrix} + \rho_2 \begin{bmatrix} 0 & 0 \\ 1 & 0 \end{bmatrix},$$

Different LPV descriptions of same nonlinear system may affect essential properties, such as controllability, observability and hence stabilizability of the system, i.e., we have different stability properties when the parameter varies freely without the connection to the state.

The nonlinear system

$$\begin{aligned} \dot{x}_1 &= -x_1 - x_1^3, \\ \dot{x}_2 &= -x_2 - x_1^2 x_2 \end{aligned}$$

can be either represented by the LPV system

$$\dot{x} = \begin{pmatrix} -1-\rho & 0 \\ 0 & -1-\rho \end{pmatrix} x, \tag{2.23}$$

with $\rho = x_1^2$, or

$$\dot{x} = \begin{pmatrix} -1-\rho_1^2+\rho_2 & -\rho_1 \\ \rho_2 & -1-\rho_1^2-\rho_1 \end{pmatrix} x, \tag{2.24}$$

with $\rho_1 = x_1$ and $\rho_2 = x_2$. In the first case it is assumed that the parameter ρ is bounded by $0 \leq \rho(t) \leq M$, where M is any fixed positive scalar; thus the nonlinear system is included in the domain $\{x \in \mathbb{R}^2 | -\sqrt{M} \leq x_1 \leq \sqrt{M}\}$. In the second case the parameter can be bounded by $-M \leq \rho_i \leq M$; thus the nonlinear system is included in the system in the domain $\{x \in \mathbb{R}^2 \mid -M \leq x_i \leq M,\ i = 1, 2\}$.

These LPV models have different properties: system (2.23) is LTI stable for all parameter values while the LPV system (2.24) is LTI unstable if $\rho_1 = 0$ and $\rho_2 > 1$. This fact out-rules constant matrix Lyapunov techniques to analyze stability of the system.

At this point it is time to recall the main goal of the LPV modeling, namely to obtain a control oriented model that facilitates the analysis and design process in the context of the available tools. At the time being these tools premises convexity, i.e., the convexity of the model set defined by the parameters Ω. Thus, the inherent non-uniqueness of the LPV modeling can be exploited in order to select those models that have this property. Moreover, in order to decrease the possible conservativeness of the design, we prefer the most compact representations.

Even the parameter set Ω is convex, it is usually not easily dealt with, since represents an infinity number of conditions. One way to overcome this difficulty is to approximate the exact set by a tractable one. By choosing appropriate inner/outer approximations one may develop computable lower/upper bounds for certain performances, e.g., stability margins.

As a possible solution, a uniformly and automatically executable tensor product (TP) model transformation method based based on the recently developed higher order singular value decomposition (HOSVD) concept has been proposed, see Zabó et al. (2008, 2010). The so called TP model transformation offers uniform, tractable and readily executable numerical ways and creative manipulations to generate convex (polytopic) representations of LPV models upon which LMI-based design techniques are immediately executable. The result of the TP model transformation is a model that belongs to the class of polytopic models, where the parameter-dependent weightings of the vertex systems are one-dimensional functions of the elements of the parameter vector.

This form offers a relatively simple way to describe various convex hull generations in terms of matrix operations. The obtained structures are not unique, however the framework provides an efficient background to introduce a set of rules, heuristics and algorithms that provide us with a set of candidate model structures on which further analysis and final model selection can be carried out.

After applying one of the modeling steps sketched in the previous sections one ends up with a parameter-varying state-space model of the form

$$\begin{pmatrix} \dot{x}(t) \\ y(t) \end{pmatrix} = S(\rho(t)) \begin{pmatrix} x(t) \\ u(t) \end{pmatrix} \tag{2.25}$$

with the parameter-varying system matrix

$$S(\rho(t)) = \begin{pmatrix} A(\rho(t)) & B(\rho(t)) \\ C(\rho(t)) & D(\rho(t)) \end{pmatrix}. \tag{2.26}$$

The time varying N-dimensional parameter vector $\rho(t) \in \Omega$ is an element of the closed hypercube $\Omega = [a_1, b_1] \times [a_2, b_2] \times \cdots \times [a_N, b_N] \subset \mathbb{R}^N$.

For practical reasons a finite element TP modeling is applied which uses a tensor defined by the values of $S(\rho(t))$ on a suitable discretization of Ω (usually a grid), i.e., a piecewise linear approximation of the multivariate map $S(\rho(t))$. Based on this data TP model transformation generates the HOSVD-based canonical form of LPV models, i.e.,

$$\begin{pmatrix} x(t) \\ y(t) \end{pmatrix} = \left(\mathcal{S} \otimes_{n=1}^{N} w_n(q_n(t)) \right) \begin{pmatrix} x(t) \\ u(t) \end{pmatrix}. \tag{2.27}$$

$\otimes_i$ denotes the i-mode tensor product as defined in Baranyi (2004), Baranyi et al. (2003).

One of the advantages of this model transformation is that it can be executed uniformly (irrespective of whether the model is given in the form of analytical equations

resulting from physical considerations, or as an outcome of soft computing based identification techniques such as neural networks or fuzzy logic based methods, or as a result of a black-box identification), without analytical interaction, within a reasonable amount of time. The obtained structure can be directly used for an LFT type modeling without any further preprocessing step.

According to defined by the ordering $(i_1, \ldots, i_N) \to r$ in the multi base number system defined by $(I_1, I_2, \ldots, I_N)$ the weighting functions are denoted by $w_r(\rho(t)) = \prod_k w_{k,i_k}(\rho_k(t)) \in [0, 1]$, where $w_{k,j}(\rho_k(t)) \in [0, 1]$ is the j-th one variable weighting function defined on the k-th dimension of Ω, while the corresponding vertex systems are $S_r = S_{i_1,i_2,\ldots,i_N}$. Using this index transformation one can write the model in the typical polytopic form:

$$S(\rho(t)) = \sum_{r=1}^{R} w_r(\rho(t)) S_r. \tag{2.28}$$

The convex hull of $S(\rho)$ might not be polytopic, however for design purposes a finite, polytopic (outer) approximation is needed. Convexity is ensured by the following conditions:

$$\forall n \in [1, N], i, \rho_n(t) : w_{n,i}(\rho_n(t)) \in [0, 1]; \tag{2.29}$$

$$\forall n \in [1, N], \rho_n(t) : \sum_{i=1}^{I_n} w_{n,i}(\rho_n(t)) = 1. \tag{2.30}$$

There are many ways to define the vertex systems and the type of the convex hull determined by the vertex system can be defined by the weighting functions. The applications of TP models specifies special requirements for the weighting functions.

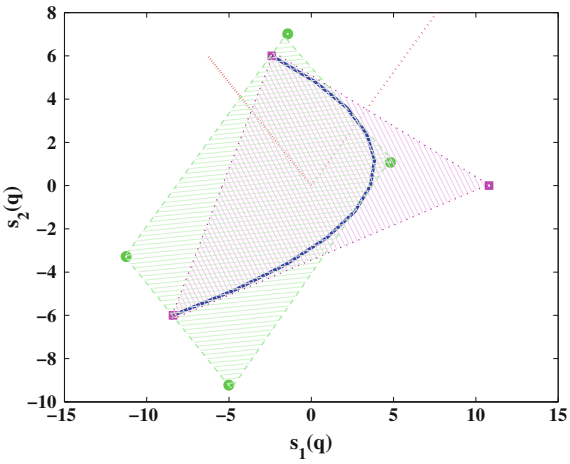


Fig. 2.2 Different convex approximations

For illustration purposes consider $S(\rho) = [\rho - \rho^2 \quad 2\rho]$ where $\rho \in [-3, 3]$. In Fig. 2.2 one can see the system $S(\rho)$ (in blue) while the dotted red lines depicts the directions given by the HOSVD while in green is depicted the smallest box that contains the convex hull $\tilde{S}$ of $S(\rho)$. Another convex hull is depicted in magenta, that corresponds to a TP model.

Often it is a non-trivial task to chose between the different model candidates. Then an important selection criteria is the solvability property of the design problems associated to the control tasks at hand.

2.3 Linearization by LFT Techniques

An LFT based model set is widely considered to be the most general representation adopted in robust controller design. From an analysis point of view the scheduling variables play the same role as the uncertainties and this fact can be reflected in the model structure. Both the Jacobian linearization and the LPV approximations lead to a parameter-dependent family of linear systems. Thus, the parameter dependence in the LPV system can be represented as an LFT. This representation provides a particular structure to the LPV system, also known as a $P - \Theta$ configuration, whereby the parameter-varying, uncertain or nonlinear terms are located in the Θ operator and the LTI part is described by the operator P.

Consider a feedback system, in which both the plant and the controller have a linear fractional dependence on Θ, see in the left-hand side of Fig. 2.3. In this representation P and K are known LTI models. The dependence of the plant and the controller are represented by the blocks Θ with input/output signals e_δ, d_δ and $\tilde{e}_\delta$, $\tilde{d}_\delta$. The block diagonal time-varying operator specifying the plant dynamics is denoted by

$$\Theta = \text{diag}(\rho_1 I_{r1}, ..., \rho_k I_{rk}), \qquad \text{where} \quad r_i > 1$$

whenever the parameter ρ_i is repeated and $r = \sum_{i=1}^{k} r_i$.

An LPV plant with a linear fractional dependence on Θ can be represented by the upper LFT interconnection:

$$\begin{bmatrix} z \\ y \end{bmatrix} = F_u(P, \Theta) \begin{bmatrix} d \\ u \end{bmatrix}. \tag{2.31}$$

The inputs and outputs of the augmented plant P is the following:

$$\left[\begin{array}{c} e_\delta \\ \hline z \\ y \end{array}\right] = \left[\begin{array}{c|cc} P_{\Theta\Theta} & P_{\Theta 1} & P_{\Theta 2} \\ \hline P_{1\Theta} & P_{11} & P_{12} \\ P_{2\Theta} & P_{21} & P_{22} \end{array}\right] \left[\begin{array}{c} d_\delta \\ \hline d \\ u \end{array}\right] \tag{2.32}$$

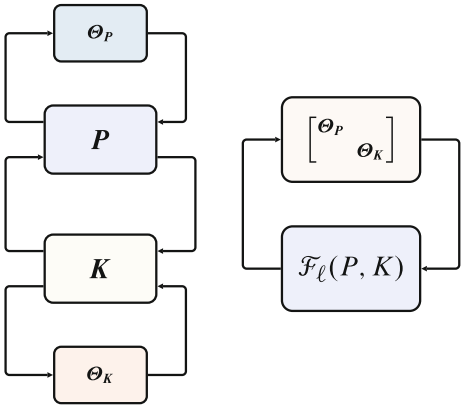


Fig. 2.3 The LPV control structure and its transformed form

Using the relation between d_δ and e_δ ($e_\delta = \Theta d_\delta$) the upper LFT interconnection structure is the following:

$$F_u(P,\Theta) = \begin{bmatrix} P_{1\Theta} \\ P_{2\Theta} \end{bmatrix} \Theta (I - P_{\Theta\Theta}\Theta)^{-1} \begin{bmatrix} P_{\Theta 1} & P_{\Theta 2} \end{bmatrix} + \begin{bmatrix} P_{11} & P_{12} \\ P_{21} & P_{22} \end{bmatrix}. \tag{2.33}$$

The feedback relation between u and y is

$$u = F_\ell(K,\Theta)y. \tag{2.34}$$

Note that while in most of the cases we use the same block Θ to schedule the plant and the controller, in general one may use blocks with a different structure. This fact is reflected in the notation of the Fig. 2.3. For the sake of simplicity in the formulas we use identical blocks.

The structure of the controller has the following relation:

$$\begin{bmatrix} u \\ \tilde{e}_\delta \end{bmatrix} = \begin{bmatrix} K_{11} & K_{1\Theta} \\ K_{\Theta 1} & K_{\Theta\Theta} \end{bmatrix} \begin{bmatrix} y \\ \tilde{d}_\delta \end{bmatrix}. \tag{2.35}$$

where the relation between d_δ and e_δ is $e_\delta = \Theta d_\delta$. The lower LFT interconnection structure is the following: $F_\ell(K,\Theta) = K_{1\Theta}\Theta(I - K_{\Theta\Theta}\Theta)^{-1}K_{\Theta 1} + K_{11}$.

The closed-loop operator from disturbance d to controlled output z is given by

$$T(P,K,\Theta) = F_\ell(F_u(P,\Theta), F_\ell(K,\Theta)). \tag{2.36}$$

The LFT structure can be transformed into a modified structure in which all parameter-dependent components are gathered into a single uncertainty block, see in the right-hand side of Fig. 2.3. Then the augmented plant is formalized in the following way:

$$\left[\begin{array}{c} \tilde{e}_\delta \\ \hline e_\delta \\ z \\ y \\ \hline \tilde{y} \end{array}\right] = \left[\begin{array}{c|c|c} 0 & 0 & I_r \\ \hline 0 & P & 0 \\ \hline I_r & 0 & 0 \end{array}\right] \left[\begin{array}{c} \tilde{d}_\delta \\ \hline d_\delta \\ d \\ u \\ \hline \tilde{u} \end{array}\right] \tag{2.37}$$

since $\tilde{y} = \tilde{d}_\delta$ and $\tilde{u} = \tilde{e}_\delta$. Here P is formalized using Eq. (2.32).

The closed-loop mapping from exogenous input d to controlled output z is expressed as

$$T(P, K, \Theta) = F_u\left(F_\ell(P_a, K), \begin{bmatrix} \Theta & 0 \\ 0 & \Theta \end{bmatrix}\right), \tag{2.38}$$

where P_a is formalized using Eq. (2.37). The original LPV problem can be viewed as a more classical robust performance problem in the face of the block-repeated uncertainty structure $\mathrm{diag}(\Theta, \Theta)$. This repeated structure is denoted by $\Delta \oplus \Delta$.

The approximation of the nonlinear system based on LFT structure is also found in Packard and Wu (1993), Packard (1994), Apkarian and Gahinet (1995).

2.4 Performance-Driven LPV Modeling

In a control design problem a control law has to be designed for a given system to reach the required performance specifications. The classical approach consists in building a mathematical model of the plant and this model is augmented with additional elements that reflect the different performance specifications. In most of the cases a given performance is modelled by the norm of a suitably selected set of signals. These signals—the performance signals—are related to the signals of the core model through some filtering. These filters are referred to as performance weights.

Recall the basic robust control paradigm: the design starts from a typical interconnection structure shown in Fig. 2.4. The Δ_m block contains the uncertainties of the system, such as unmodelled dynamics and parameter uncertainty. In this augmented plant unmodelled dynamics is represented by a weighting function W_r and a block Δ_m. The purpose of the weighting functions W_w and W_n is to reflect the disturbance and sensor noises.

In this framework performance requirements are imposed to signals z through a suitable choice of the weighting functions W_p. In contrast to the weights associated to control inputs and uncertainties, the role of these filters is not only to scale the signals but also to ensure a desired frequency separation between competing requirements, see, e.g., tracking and robustness. Thus, the performance weights are usually some dynamical systems, in a pure LTI setting transfer functions. In what follows we first list some of the typical control goals and the associated signals that are encountered in design problems.

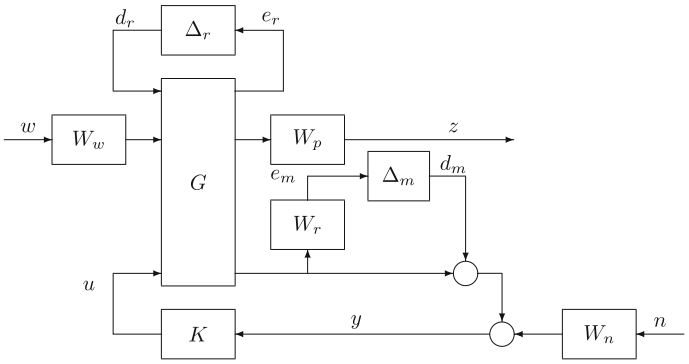


Fig. 2.4 The closed-loop interconnection structure

Yaw stability can be achieved by limiting the effects of the lateral load transfers. Then, the purpose of the control design is to minimize the lateral acceleration $z_a = a_y$, which can be chosen as a performance signal. Another control task is road tracking, i.e., to follow the road geometry. The purpose of the control is to minimize the difference between the yaw rate and the reference yaw rate: $z_e = |\psi_{act} - \psi_{ref}|$.

Roll stability is achieved by limiting the lateral load transfers on both axles to below the levels for wheel lift-off during various vehicle maneuvers. The lateral load transfer is $\Delta F_{zi} = k_t \phi_{ti}$, where ϕ_{ti} is the monitored roll angle of the unsprung mass at the front and the rear. The normalized lateral load transfer is introduced as $\rho_R = \Delta F_{zy}/(mg)$ and the aim of the control design is to reduce the maximum value of the normalized lateral load transfer if it exceeds a predefined critical value.

The pitch angle of the sprung mass may increase significantly during a sudden and hard braking. Thus a pitch stability requirement can be introduced which is achieved by limiting the longitudinal load transfers to below a predefined level. The normalized longitudinal load transfer is the normalized value of the pitch angle: $\rho_P = \theta/\theta_{max}$ where θ is the monitored pitch angle and θ_{max} is the maximal value of the pitch angle. The aim of the control design during braking is to reduce the pitching dynamics if the normalized longitudinal load transfer exceeds a critical value.

Finally, the control problem can be formulated in the general P-K-Δ structure, where P is the generalized plant and Δ contains both the uncertainties and the scheduling variables. In the design of local controllers the quadratic LPV performance problem is to choose the parameter-varying controller in such a way that the resulting closed-loop system is quadratically stable and the induced $\mathscr{L}_2$ norm from the disturbance and the performances is less than the value γ. The minimization task is the following (Fig. 2.5):

$$\inf_{K} \sup_{\Delta} \sup_{\|w\|_2 \neq 0, w \in \mathscr{L}_2} \frac{\|z\|_2}{\|w\|_2}. \tag{2.39}$$

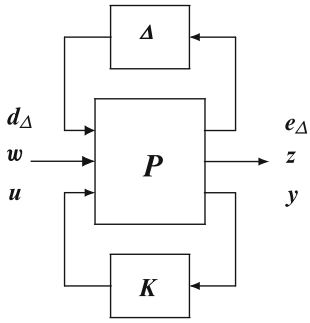


Fig. 2.5 The $P - K - \Delta$ structure

Nowadays there is a growing demand for vehicles with ever better driving characteristics in which efficiency, safety, and performance are ensured. In line with the requirements of the vehicle industry several performance specifications are in the focus of research, e.g., improving road holding, passenger comfort, roll and pitch stability, guaranteeing the reliability of vehicle components, reducing fuel consumption and proposing fault-tolerant solutions. An integrated control system is designed in such a way that the effects of a control system on other vehicle functions are taken into consideration in the design process by selecting the various performance specifications.

In a multi-layer supervisory architecture for integrated control systems the supervisor has information about the various vehicle maneuvers and the different fault operations by monitoring components and FDI filters. Thus, it is able to make decisions about the necessary interventions into the vehicle components and guarantee the reconfigurable and fault-tolerant operation of the vehicle. The role of the supervisor is to meet performance specifications and avoid the interference and conflict between components.

The advantage of the architecture for integrated vehicle control is that the complexity of the vehicle model is divided into several parts. In the formalism of the control-oriented model the messages of the supervisor must be taken into consideration. Consequently, the signals of monitoring components and FDI filters are built in the performance specifications of the controller by using parameter-dependent weighting. In this way the operation of a local controller can be extended to reconfigurable and fault-tolerant functions.

In the supervisory decentralized control the role of LPV methods is fundamental. In the formalism of the control oriented model, the selection of monitoring components and building them into signals, which are related to the performance requirements, are crucial points in the modeling. The proposed approach realizes the reconfiguration of the performance objectives by an appropriate scheduling of the corresponding weighting functions.

To illustrate the idea: consider a suspension system design where the performance weighting functions for heave acceleration and suspension deflections are selected as

$$W_{p,az} = \phi_{az} W_{0,az},$$
$$W_{p,sd} = \phi_{sd} W_{0,sd},$$

where ϕ_{az} and ϕ_{sd} are parameter varying gains. A large gain ϕ_{az} and a small gain ϕ_{sd} correspond to a design that emphasizes passenger comfort while choosing ϕ_{az} small and ϕ_{sd} large corresponds to a design that focuses on suspension deflection. A possible modeling choice is to select the suspension deflection as the parameter ρ that schedules these gains.

In order to sketch a possible choice for these scheduling variables two parameters are defined: c_1 and c_2. When the suspension deflection d is below c_1, the gain ϕ_a is selected to be constant and the gain ϕ_d is zero. When the deflection is between c_1 and c_2 the gains change linearly. When the value of the suspension deflection is greater than c_2, the gain ϕ_d is constant and the gain ϕ_a is zero, see Fig. 2.6.

We emphasize that in this way we obtain an LPV model and place the design into the LPV framework, even the original plant was modeled as an LTI system.

Since fault-tolerant control requires fault information in order to guarantee performances and modify its operation the presence of suitably designed FDI filters are needed. Then, the fault information provided by the FDI filter can be quantified as $\rho_D = f_{act}/f_{max}$, where f_{act} is an estimation of the failure (output of the FDI filter), that means the rate of the performance degradation of an active component, and f_{max} is an estimation of the maximum value of the potential failure (fatal error). Thus, the value of a possible fault is normalized into the interval $\rho_D = [0,\ 1]$.

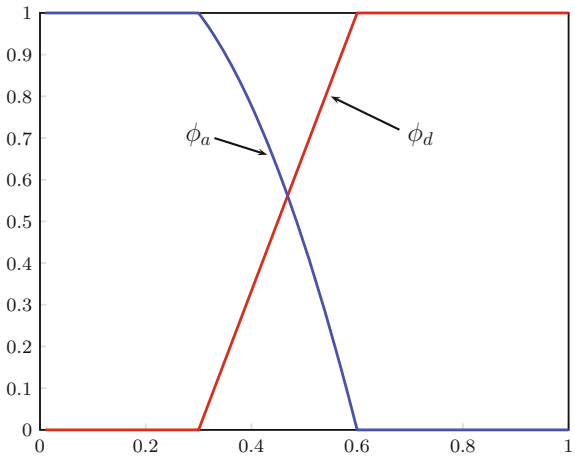


Fig. 2.6 Gains of the performance weights: ϕ_a and ϕ_d

The actuator reconfiguration is based on the fact that two actuators are able to influence the same vehicle dynamics. Thus, the fault-free actuator it is able to substitute for the operation of another actuator which has been affected by a failure or its performance has degraded. The control design is based on two factors: the failure or performance degradation have already been detected and the fault information ρ_D and the necessary intervention possibilities are built into its control design. This goal is achieved by a suitable scheduling of the corresponding W_p performance and W_a actuator weights.

As an example consider the design of the brake system the command signal is the difference in brake forces while the performance signal is the lateral acceleration: $z_b = \left[a_y, u_r\right]^T$. The weighting function of the lateral acceleration is selected as:

$$W_{pa} = \phi_a W_{0,pa},$$

where ϕ_a is a gain, which reflects the relative importance of the lateral acceleration and it is chosen to be parameter-dependent, e.g., the function of the normalized lateral load transfer ρ_R. When the vehicle is not in an emergency ρ_R is small ($|\rho_R| < R_b$), i.e., ϕ_a is small, indicating that the LPV control should not focus on minimizing acceleration. On the other hand, when ρ_R approaches the critical value, i.e., when $|\rho_R| \geqq R_b$, ϕ_a is large, it indicates that the control should focus on preventing the rollover.

Here the fixed parameter R_b defines the critical status when the vehicle is close to the rollover situation, i.e., all wheels are on the ground but the lateral tire force of the inner wheels tends to zero. Moreover, a parameter R_a can also be introduced to reflect how fast the control should focus on minimizing the lateral acceleration. These parameters guarantee the smooth transient of the signals, e.g., for the following choice:

$$\phi_a = \begin{cases} 1 & \text{if} \quad |\rho_R| > R_b \\ \frac{|\rho_R| - R_a}{R_b - R_a} & \text{if} \quad R_a \leq |\rho_R| \leq R_b \\ 0 & \text{if} \quad |\rho_R| < R_a \end{cases}$$

Moreover, in the presence of an anti-roll bar system, if a fault is detected in the operation of the anti-roll bars the brake system will be activated at a smaller critical value than in a fault-free case, i.e., when $|\rho_{Da}| > 0$. Consequently, the brake is activated in a modified way and the brake moment is able to assume the role of the anti-roll bars or the suspension actuator in which the fault has occurred. The modified critical value is

$$R_{a,new} = R_a - \alpha \cdot \rho_{Da},$$

where α is a predefined constant factor.

2.5 LPV Modeling of Two Subsystems

2.5.1 Modeling of the Vertical Dynamics

The full-car vehicle model, which is shown in Fig. 2.7, comprises five parts: the sprung mass and four unsprung masses. Let the sprung and unsprung masses be denoted by m_s, m_{uf}, and m_{ur}, respectively. All suspensions consist of a spring, a damper and an actuator, which generates a pushing force between the body and the axle. The front and rear suspension stiffnesses, the front and rear tire stiffnesses are denoted by k_{sf}, k_{sr}, and k_{tf}, k_{tr}, respectively. The front and rear suspension dampings are denoted by b_{sf}, b_{sr}, respectively. Let the front and rear displacement of the sprung mass on the left and right side be denoted by x_{1fl}, x_{1rl} and x_{1fr}, x_{1rr}, respectively. Let the front and rear displacement of the unsprung mass on the left and right side be denoted by $x_{2fl}, x_{2rl}, x_{2fr}$, and x_{2rr}, respectively. In the full-car model, the disturbances, $w_{fl}, w_{rl}, w_{fr}, w_{rr}$ are caused by road irregularities. The control forces, $F_{zfl}, F_{zrl}, F_{zfr}, F_{zrr}$ are generated by the actuators.

The full-car model is based on a seven degrees of freedom system. The sprung mass is assumed to be a rigid body and has freedoms of motion in the vertical, pitch and roll directions. Accordingly: x_1 is the vertical displacement at the center of gravity, θ is the pitch angle and ϕ is the roll angle of the sprung mass. The following linear approximations are applied to the front and rear displacements of the sprung mass on the left and right side:

$$\begin{aligned} x_{1fl} &= x_1 + \ell_f\theta + t_f\phi, \\ x_{1fr} &= x_1 + \ell_f\theta - t_f\phi, \\ x_{1rl} &= x_1 - \ell_r\theta + t_r\phi, \\ x_{1rr} &= x_1 - \ell_r\theta - t_r\phi. \end{aligned}$$

In the following the first principle based motion equations are formalized using the Lagrangian mechanics. Since in the model there exist seven degrees of freedom, define the generalized coordinates as

$$q = \left[x_1\ \theta\ \phi\ x_{2fl}\ x_{2fr}\ x_{2rl}\ x_{2rr}\right]^T. \tag{2.40}$$

When the kinetic energy for a moving rigid body is calculated from both the oscillation of the vehicle body and the vertical displacements of unsprung components are taken into consideration. Since the yaw motion compared to the steering movement is ignored and the roll angle is assumed to be small, the angular velocities are approximated in the following way:

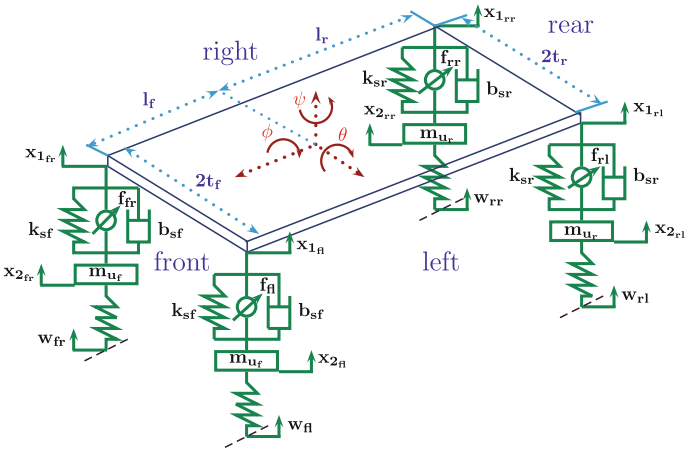


Fig. 2.7 The vertical dynamics of a full-car model

$$\Omega_x = \dot{\theta} sin\phi \approx 0,$$
$$\Omega_y = \dot{\theta} cos\phi \approx \dot{\theta},$$
$$\Omega_z = \dot{\phi}.$$

Thus, the kinetic energies contributed from the vehicle body and the unsprung components:

$$T_B = \frac{1}{2} M_s \dot{x}_1^2 + \frac{1}{2} I_\theta \dot{\theta}^2 + \frac{1}{2} I_\phi \dot{\phi}^2, \tag{2.41}$$
$$T_U = \frac{1}{2} m_{uf} (\dot{x}_{2fl}^2 + \dot{x}_{2fr}^2) + \frac{1}{2} m_{ur} (\dot{x}_{2rl}^2 + \dot{x}_{2rr}^2) \tag{2.42}$$

and the total kinetic energy is $T = T_B + T_U$.

The potential energy includes the deformations of springs and tires of the vehicle during vibrations. The deformations of the tires and that of the suspension components are:

$$d_{2fl} = x_{2fl} - w_{fl}, \quad d_{2fr} = x_{2fr} - w_{fr}, \quad d_{2rl} = x_{2rl} - w_{rl}, \quad d_{2rr} = x_{2rr} - w_{rr},$$

and

$$d_{1fl} = x_{1fl} - x_{2fl}, \quad d_{1fr} = x_{1fr} - x_{2fr}, \quad d_{1rl} = x_{1rl} - x_{2rl}, \quad d_{1rr} = x_{1rr} - x_{2rr},$$

respectively. The potential energy is the sum of two components: $U = U_S + U_T$, where U_S contains the potential energy stored in suspension systems and U_T contains the potential energy stored in tires:

$$U_S = \frac{1}{2}k_{sf}(d_{1fl}^2 + d_{1fr}^2) + \frac{1}{2}k_{sr}(d_{1rl}^2 + d_{1rr}^2), \tag{2.43}$$

$$U_T = \frac{1}{2}k_{tf}(d_{2fl}^2 + d_{2fr}^2) + \frac{1}{2}k_{tr}(d_{2rl}^2 + d_{2rr}^2). \tag{2.44}$$

The dissipation energy accounts for the effect of shock absorbers. Assuming that the forces produced by dampers vary linearly with the rates of change of deformations, the dissipation function is obtained as

$$D = \frac{1}{2}b_{sf}(\dot{d}_{1fl}^2 + \dot{d}_{1fr}^2) + \frac{1}{2}b_{sr}(\dot{d}_{1rl}^2 + \dot{d}_{1rr}^2). \tag{2.45}$$

The external forces are formalized for all generalized coordinates:

$$f_1 = -F_{zfl} - F_{zfr} - F_{zrl} - F_{zrr}, \quad f_2 = -l_f F_{zfl} - l_f F_{zfr} + l_r F_{zrl} + l_r F_{zrr}, \quad f_4 = F_{zfl},$$
$$f_3 = -t_f F_{zfl} + t_f F_{zfr} - t_r F_{zrl} + t_r F_{zrr}, \quad f_5 = F_{zfr}, \quad f_6 = F_{zrl} \text{ and } f_7 = F_{zrr}.$$

Then the Lagrangian equations of the full-car model are formalized as follows.

$$M_s\ddot{q} = LB_s(\dot{x}_u - \dot{x}_s) + LK_s(x_u - x_s) - Lf, \tag{2.46}$$

$$M_u\ddot{x}_u = B_s(\dot{x}_s - \dot{x}_u) + K_s(x_s - x_u) + K_t(w - x_u) + f, \tag{2.47}$$

where $q = \begin{bmatrix} x_1 & \theta & \phi \end{bmatrix}^T$, $x_s = \begin{bmatrix} x_{1fl} & x_{1fr} & x_{1rl} & x_{1rr} \end{bmatrix}^T$, $x_u = \begin{bmatrix} x_{2fl} & x_{2fr} & x_{2rl} & x_{2rr} \end{bmatrix}^T$, $w = \begin{bmatrix} w_{fl} & w_{fr} & w_{rl} & w_{rr} \end{bmatrix}^T$, and $f = \begin{bmatrix} F_{zfl} & F_{zfr} & F_{zrl} & F_{zrr} \end{bmatrix}^T$. The sprung mass ($M_s$), the unsprung mass ($M_u$), the suspension stiffness (K_s), the tire stiffness (K_t), suspension damping (B_s), geometry (L) matrices can be formulated as follows:

$$M_s = \begin{bmatrix} m_s & 0 & 0 \\ 0 & I_\theta & 0 \\ 0 & 0 & I_\phi \end{bmatrix}, \quad M_u = \begin{bmatrix} m_{uf} & 0 & 0 & 0 \\ 0 & m_{uf} & 0 & 0 \\ 0 & 0 & m_{ur} & 0 \\ 0 & 0 & 0 & m_{ur} \end{bmatrix}, \quad B_s = \begin{bmatrix} b_{sf} & 0 & 0 & 0 \\ 0 & b_{sf} & 0 & 0 \\ 0 & 0 & b_{sr} & 0 \\ 0 & 0 & 0 & b_{sr} \end{bmatrix},$$

$$K_s = \begin{bmatrix} k_{sf} & 0 & 0 & 0 \\ 0 & k_{sf} & 0 & 0 \\ 0 & 0 & k_{sr} & 0 \\ 0 & 0 & 0 & k_{sr} \end{bmatrix}, \quad K_t = \begin{bmatrix} k_{tf} & 0 & 0 & 0 \\ 0 & k_{tf} & 0 & 0 \\ 0 & 0 & k_{tr} & 0 \\ 0 & 0 & 0 & k_{tr} \end{bmatrix}, \quad L = \begin{bmatrix} 1 & 1 & 1 & 1 \\ l_f & l_f & -l_r & -l_r \\ t_f & -t_f & t_r & -t_r \end{bmatrix}.$$

The nominal parameters of the full-car model are in Table 2.1.

Using the kinematic relationship between x_s and q:

$$x_s = L^T q \tag{2.48}$$

and by substituting Eq. (2.48) for Eq. (2.46), the following differential equation is formalized:

Table 2.1 Parameters of the full-car model

Parameters (symbols)	Value	Unit
Sprung mass (m_s)	1400	kg
Pitch moment inertia (I_θ)	2100	kg m^2
Roll moment inertia (I_ϕ)	460	kg m^2
Unsprung masses (m_{uf}, m_{ur})	40, 40	kg
Suspension stiffness (k_{sf}, k_{sr})	23500, 25500	N/m
Front tire stiffness (k_{tf}, k_{tr})	190000, 190000	N/m
Suspension damping (b_{sf}, b_{sr})	1000, 1100	N/m/s
Actuator parameters (α, β, γ),	$4.515 \cdot 10^{13}$, 1, $4.969 \cdot 10^{12}$	
Area of piston (A_P)	$3.35 \cdot 10^{-4}$	m^2
Supply pressure (P_s)	10342500	Pa
Time constant (τ)	$\frac{1}{30}$	s

$$M\ddot{z} + B\dot{z} + Kz = K_r w + L_a f, \tag{2.49}$$

where $z = \begin{bmatrix} q^T & x_u^T \end{bmatrix}^T$, and the matrices are as follows:

$$M = \begin{bmatrix} M_s & 0 \\ 0 & M_u \end{bmatrix}, \quad B = \begin{bmatrix} LB_sL^T & -LB_s \\ -B_sL^T & B_s \end{bmatrix},$$
$$K = \begin{bmatrix} LK_sL^T & -LK_s \\ -K_sL^T & K_s + K_t \end{bmatrix}, \quad K_r = \begin{bmatrix} 0 \\ K_t \end{bmatrix}, \quad L_a = \begin{bmatrix} -L \\ I \end{bmatrix}.$$

Equation (2.49) can be represented as a state space form:

$$\dot{x} = Ax + B_1 w + B_2 u, \tag{2.50}$$

where $x = \begin{bmatrix} z^T & \dot{z}^T \end{bmatrix}^T$, $u = f$ and

$$A = \begin{bmatrix} 0 & I \\ -M^{-1}K & -M^{-1}B \end{bmatrix}, \quad B_1 = \begin{bmatrix} 0 \\ M^{-1}K_r \end{bmatrix}, \quad B_2 = \begin{bmatrix} 0 \\ M^{-1}L_a \end{bmatrix}.$$

The nominal parameters of the full-car model are in Table 2.1. From disturbances to performance signals the open-loop frequency responses of the full-car model, i.e., the heave, pitch, roll accelerations and suspension deflections, are illustrated in Fig. 2.8.

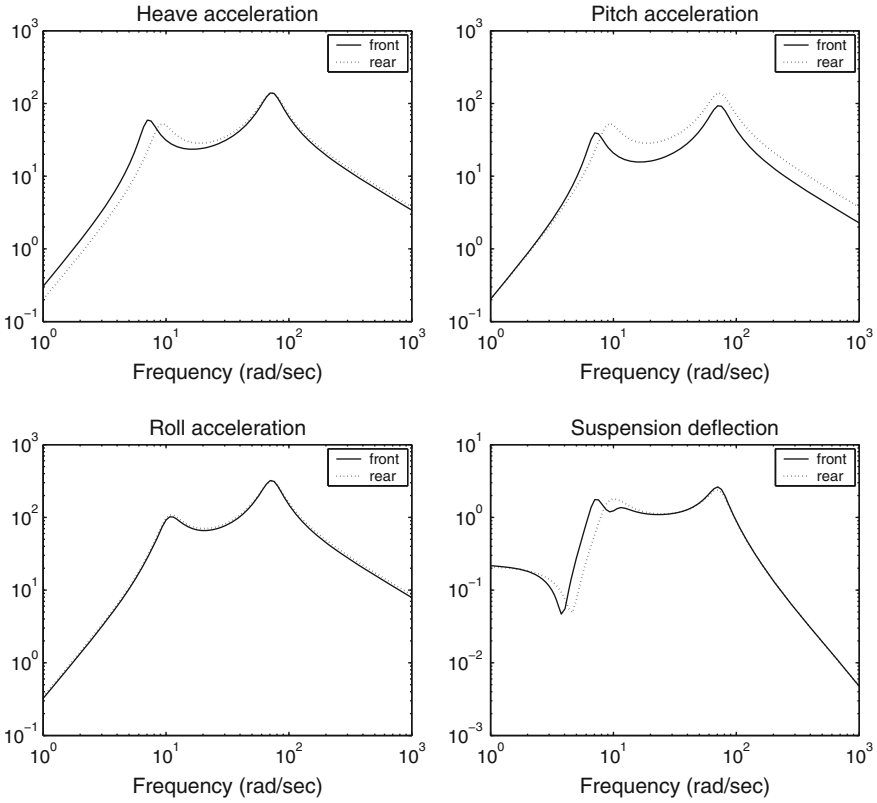


Fig. 2.8 Frequency responses of the full-car model to disturbances

2.5.2 Nonlinear Components of the Vertical Dynamics

In the full-char model presented in the previous section it was not explicitly expressed the nonlinearity of the suspension stiffness (K_s), the tire stiffness (K_t) and that of the suspension damping (B_s). Moreover the nonlinearity of the actuator was completely ignored. In what follows, we concentrate on these nonlinearities by developing the model of a relevant subsystem, the quarter-car.

The quarter-car vehicle model, which is shown in Fig. 2.9, is a two-degree-of-freedom model. $x_1 = q_1$ and $x_2 = q_2$ denote the vertical displacement of the sprung mass and the unsprung mass, respectively. In the modelling of suspension systems the nonlinear behavior of suspension components and the actuator dynamics are taken into consideration. The vertical dynamics of the suspension system is formalized in the following way:

$$m_s\ddot{x}_1 = F_{ks} + F_{bs} - F_{az}, \tag{2.51}$$

$$m_u\ddot{x}_2 = -F_{ks} - F_{bs} - k_t(x_2 - w) + F_{az}, \tag{2.52}$$

where F_{bs} is the suspension damping force, F_{ks} is the suspension spring force and F_{az} is the force of the actuator.

The force equation of the suspension stiffness is

$$F_{ks} = k_s^l(x_2 - x_1) + k_s^{nl}(x_2 - x_1)^3, \tag{2.53}$$

where parts of the nonlinear suspension stiffness (k_s) are a linear coefficient k_s^l and a nonlinear coefficient k_s^{nl}. The force equation of the suspension damping is

$$F_{bs} = b_s^l(\dot{x}_2 - \dot{x}_1) - b_s^{sym}(\dot{x}_2 - \dot{x}_1)sgn(\dot{x}_2 - \dot{x}_1) + b_s^{nl}\sqrt{|\dot{x}_2 - \dot{x}_1|}sgn(\dot{x}_2 - \dot{x}_1), \tag{2.54}$$

where $\dot{x}_1$ and $\dot{x}_2$ denote the vertical velocity of the sprung mass and the unsprung mass, respectively. Here, the nonlinear suspension damping b_s consists of a linear coefficient b_s^l and two nonlinear coefficients b_s^{nl} and b_s^{sym}. b_s^{nl} shows the nonlinear impact on the damping characteristics while b_s^{sym} describes its asymmetric behavior. Note that in the modelling of the suspension system a linearized model is often used instead of a nonlinear one. In the linearized version of the suspension system $F_{ks} = k_s^l(x_2 - x_1)$ and $F_{bs} = b_s^l(\dot{x}_2 - \dot{x}_1)$ are applied.

The hydraulic actuator operates nonlinearly, thus its force should be formalized in the following way, see Merritt (1967). The hydraulic actuator is controlled by electro-hydraulic servo-valves and is mounted parallel to the passive suspension system. Consider a four-way valve-piston system in which the force balance at the piston gives:

$$F_{az} = A_P P_L, \tag{2.55}$$

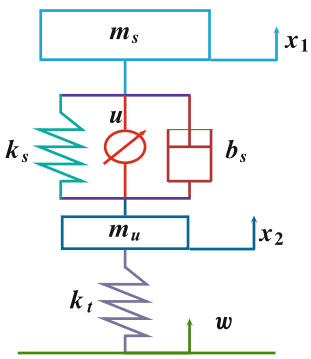


Fig. 2.9 Vertical dynamics of a quarter-car model

where A_P is the area of the piston and P_L is the pressure drop across the piston with respect to the front and rear suspensions. The derivative of P_L is given by

$$\dot{P}_L = -\beta P_L + \alpha A_P(\dot{x}_2 - \dot{x}_1) + \alpha Q, \tag{2.56}$$

in which $\alpha = \frac{4\beta_e}{V_t}$, $beta = \alpha C_{tp}$ and

$$Q = sgn[P_s - sgn(x_v)P_L]C_d S x_v \sqrt{\frac{1}{\bar{\rho}}|P_s - sgn(x_v)P_L|}, \tag{2.57}$$

and V_t is the total actuator volume, β_e is the effective bulk modulus of system, Q is the hydraulic load flow, C_{tp} is the total leakage coefficient of the piston, C_d is the discharge coefficient, S is the spool valve area gradient, x_v is the displacement of the spool valve, $\bar{\rho}$ is the hydraulic fluid density, P_s is the supply pressure. The cylinder velocity acts as a coupling from the position output of the cylinder to the pressure differential across the piston. It is considered a feedback term, which has been analyzed by Alleyne and Hedrick (1992), Alleyne and Liu (2000). The displacement of the spool valve x_v is controlled by the input to the servo-valve u:

$$\dot{x}_v = \frac{1}{\tau}(-x_v + u). \tag{2.58}$$

The state space representation of the nonlinear model is:

$$\dot{x} = f(x) + gu + hw, \tag{2.59}$$

in which the state vector x is as follows:

$$x = \begin{bmatrix} x_1 & x_2 & x_3 & x_4 & x_P & x_v \end{bmatrix}^T. \tag{2.60}$$

The components of the state vector are the vertical displacement of the sprung mass x_1, the vertical displacement of the unsprung mass x_2, their derivatives $x_3 = \dot{x}_1$, $x_4 = \dot{x}_2$, the pressure drop $x_P (= P_L)$, and the servo valve displacement x_v. The components of the Eq. (2.59) are

$$f(x) = \begin{bmatrix} x_3 \\ x_4 \\ \frac{1}{m_s}\left(F_{ks} + F_{bs} - A_P x_P\right) \\ \frac{1}{m_u}\left(-F_{ks} - F_{bs} - k_t x_2 + A_P x_P\right) \\ -\beta x_P + \alpha A_P(x_4 - x_3) + \alpha Q \\ -\frac{1}{\tau}x_v \end{bmatrix}, \quad g = \begin{bmatrix} 0 \\ 0 \\ 0 \\ 0 \\ 0 \\ \frac{1}{\tau} \end{bmatrix}, \quad h = \begin{bmatrix} 0 \\ 0 \\ 0 \\ \frac{k_t}{m_u} \\ 0 \\ 0 \end{bmatrix}.$$

In the following, an LPV model is constructed by selecting three scheduling variables, i.e., the square of the relative displacement, the signum of the relative velocity and a signal linked to the load pressure of the actuator.

$$\rho_{ks} = (x_2 - x_1)^2, \tag{2.61}$$

$$\rho_b = sgn(x_4 - x_3), \tag{2.62}$$

$$\rho_Q = sgn[P_s - sgn(x_v)P_L]C_d S\sqrt{\frac{1}{\bar{\rho}}|P_s - sgn(x_v)P_L|}. \tag{2.63}$$

Substituting ρ_Q into equation of the actuator (2.56), the differential equation is:

$$\dot{x}_P(\rho_Q) = -\beta x_P + \alpha A_P(x_4 - x_3) + \alpha\rho_Q x_v. \tag{2.64}$$

The parameter dependence of the load pressure differential equation is affine in ρ_Q. As a consequence of affine parameter dependence, quadratic stability and control performance are guaranteed in the whole parameter region, solving an optimization problem only at extreme points in the parameter region over the LMI constraints.

The nonlinear spring force is reformulated in the following way:

$$F_{ks}(\rho_{ks}) = k_s^l(x_2 - x_1) + k_s^{nl}\rho_{ks}(x_2 - x_1). \tag{2.65}$$

This force is expressed by a linear combination of states allowing the force to have nonlinear ρ_{ks} dependence. The nonlinear damping force is partitioned in the following way:

$$F_{bs}(\rho_b) = b_s^l(x_4 - x_3) - b_s^{sym}\rho_b(x_4 - x_3) + b_s^{nl}\rho_b\sqrt{\rho_b(x_4 - x_3)}, \tag{2.66}$$

where the first and the second terms are the linear parts and the third term is the nonlinear part of the damping force. The linear parts of the damping force can be expressed as a linear combination of the states, however, the the nonlinear part cannot. Thus, a fictitious signal u_{fict} must be introduced, and the nonlinear parts must be incorporated into the disturbance matrix when the LPV model is formalized.

In the LPV model of the active suspension system three parameters are selected. In practice, the relative displacement is a measured signal. The relative velocity is then determined by numerical differentiation from the measured relative displacement. The scheduling variable ρ_Q is linked to the load pressure of the actuator, which is assumed to be calculated directly from Eq. (2.57).

The state space representation of the LPV model is as follows:

$$\dot{x} = A(\rho)x + gu + \tilde{h}\tilde{w}, \tag{2.67}$$

where $\rho = [\rho_1\ \rho_2\ \rho_3]^T$ with $\rho_1 = \rho_{ks}, \rho_2 = \rho_b, \rho_3 = \rho_Q$ and $\tilde{w} = [w\ u_{fict}]^T$ includes both the disturbance and the fictitious signals. The matrix A is expressed in the following form

Table 2.2 Parameters of the quarter-car model

Parameters (symbols)	Value	Unit
Sprung mass (m_s)	290	kg
Unsprung mass (m_u)	40	kg
Suspension stiffness (k_s^l, k_s^{nl})	$235 \cdot 10^2, 235 \cdot 10^4$	N/m
Tire stiffness (k_t)	$190 \cdot 10^3$	N/m
Damping ($b_s^l, b_s^{nl}, b_s^{sym}$)	700, 400, 400	N/m/s
Time constant (τ)	$\frac{1}{30}$	s

$$
\begin{aligned}
A(\rho) &= A_0 + \rho_1 A_1 + \rho_2 A_2 + \rho_3 A_3 \\
&= \begin{bmatrix}
0 & 0 & 1 & 0 & 0 & 0 \\
0 & 0 & 0 & 1 & 0 & 0 \\
-\frac{k_s^l}{m_s} & \frac{k_s^l}{m_s} & -\frac{b_s^l}{m_s} & \frac{b_s^l}{m_s} & -\frac{A_P}{m_s} & 0 \\
\frac{k_s^l}{m_u} & -\frac{k_s^l}{m_u} - \frac{k_t}{m_u} & \frac{b_s^l}{m_u} & -\frac{b_s^l}{m_u} & \frac{A_P}{m_u} & 0 \\
0 & 0 & -\alpha A_P & \alpha A_P & -\beta & 0 \\
0 & 0 & 0 & 0 & 0 & -\frac{1}{\tau}
\end{bmatrix} + \rho_1 \begin{bmatrix}
0 & 0 & 0\,0\,0\,0 \\
0 & 0 & 0\,0\,0\,0 \\
-\frac{k_s^{nl}}{m_s} & \frac{k_s^{nl}}{m_s} & 0\,0\,0\,0 \\
\frac{k_s^{nl}}{m_u} & -\frac{k_s^{nl}}{m_u} & 0\,0\,0\,0 \\
0 & 0 & 0\,0\,0\,0 \\
0 & 0 & 0\,0\,0\,0
\end{bmatrix} \\
&+ \rho_2 \begin{bmatrix}
0\,0 & 1 & 0 & 0\,0 \\
0\,0 & 0 & 1 & 0\,0 \\
0\,0 & \frac{b_s^{sym}}{m_s} & -\frac{b_s^{sym}}{m_s} & 0\,0 \\
0\,0 & -\frac{b_s^{sym}}{m_u} & \frac{b_s^{sym}}{m_u} & 0\,0 \\
0\,0 & 0 & 0 & 0\,0 \\
0\,0 & 0 & 0 & 0\,0
\end{bmatrix} + \rho_3 \begin{bmatrix}
0\,0\,0\,0\,0 & 0 \\
0\,0\,0\,0\,0 & 0 \\
0\,0\,0\,0\,0 & 0 \\
0\,0\,0\,0\,0 & 0 \\
0\,0\,0\,0\,0 & \alpha\rho_Q \\
0\,0\,0\,0\,0 & 0
\end{bmatrix}
\end{aligned}
$$

and components g and $\tilde{h}$ are the following:

$$
g = \begin{bmatrix} 0 \\ 0 \\ 0 \\ 0 \\ 0 \\ \frac{1}{\tau} \end{bmatrix}, \quad \tilde{h} = \begin{bmatrix}
0 & 0 \\
0 & 0 \\
0 & \frac{1}{m_s} b_s^{nl} \rho_b \sqrt{\rho_b (x_4 - x_3)} \\
\frac{k_t}{m_u} & -\frac{1}{m_u} b_s^{nl} \rho_b \sqrt{\rho_b (x_4 - x_3)} \\
0 & 0 \\
0 & 0
\end{bmatrix}.
$$

The nominal parameters are in Table 2.2.

The performance signals of the suspension system, i.e., the heave acceleration of the sprung mass, suspension deflection, wheel displacement and the control force, are tested in two examples. The excitation signals are a bump on the road surface and a square wave input.

Firstly, the performance signals of the suspension system are tested by using a bump. The performance signals are illustrated in Fig. 2.10. The overshoots of the heave acceleration are larger about 10 % in the nonlinear case than in the linear one,

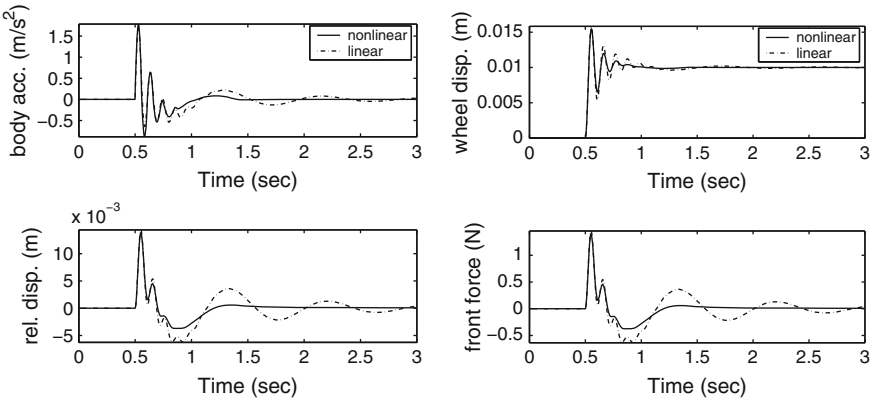


Fig. 2.10 Time responses of the vehicle to a bump

however, the transient duration of the nonlinear case is shorter than in the linear one. At the same time the values of suspension deflections are smaller in the nonlinear case than in the linear one. These properties are caused by the nonlinear damping characteristics, which are significantly different from the linear characteristics around the equilibrium point.

2.5.3 LPV Modeling of the Yaw–Roll Dynamics

The motion differential equations, i.e., the lateral dynamics, the yaw moment, the roll moment of the sprung mass, the roll moment of the front and the rear unsprung masses are the following. These equations were also formulated in Sampson and Cebon (2003), Gáspár et al. (2005c).

Figure 2.11 illustrates the combined yaw–roll dynamics of a vehicle, which is modelled by a three-body system, in which m_s is the sprung mass, $m_{u,f}$ is the unsprung mass at the front including the front wheels and axle, $m_{u,r}$ is the unsprung mass at the rear with the rear wheels and axle, and m is the total vehicle mass.

I_{xx}, I_{xz}, I_{zz} are the roll moments of the inertia of the sprung mass, the yaw–roll product, and the yaw moment of inertia, respectively. h is the height of CG of sprung mass and $h_{u,f}$, $h_{u,r}$ are the height of CG of unsprung masses and r is the height of the roll axis from ground. The total axle loads are F_{zl} and F_{zr}, respectively.

The roll motion of the sprung mass is damped by suspensions with damping coefficients b_{sf}, b_{sr} and stiffness coefficients k_{sf}, k_{sr}. The tire stiffnesses are denoted by k_{tf} and k_{tr}. The signals are the forward velocity v,the lateral acceleration a_y, the side slip angle of the sprung mass β, the heading angle ψ, the yaw rate $\dot{\psi}$, the roll angle ϕ, the roll rate $\dot{\phi}$, the roll angle of the unsprung mass at the front axle $\phi_{t,f}$ and at the rear axle $\phi_{t,r}$.

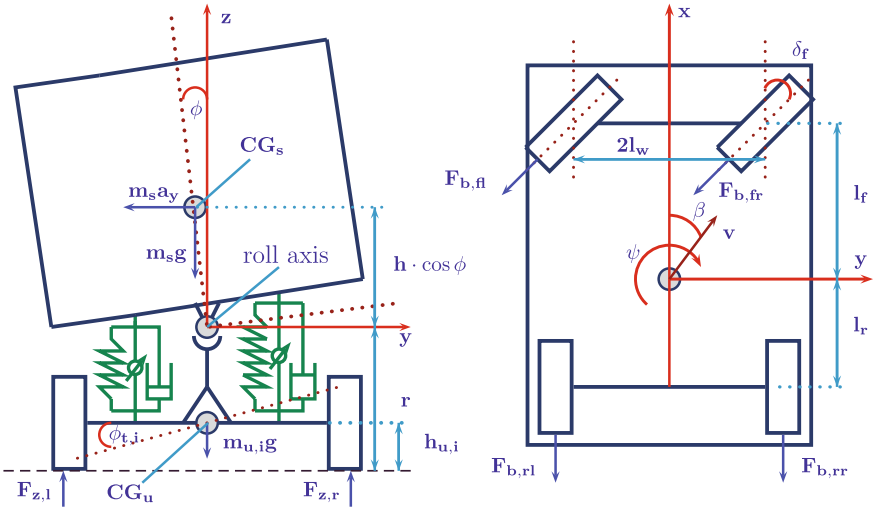


Fig. 2.11 Illustration of the vehicle model

δ_f is the front wheel steering angle and ΔF_b are the braking forces on the left and right hand side wheels. It is assumed that the difference between the brake forces ΔF_b provided by the compensator is applied to the rear axle. This assumption does not restrict the implementation of the compensator because it is possible that the control action be distributed at the front and the rear wheels at either of the two sides.

In vehicle modelling the motion differential equations of the combined yaw and roll dynamics of the single unit vehicle are formalized. The vehicle can translate longitudinally and laterally and it can also yaw. The sprung mass can rotate around a horizontal axis. The unsprung masses can also roll, permitting the vertical compliance of the tires. The motion is described using a coordinate system fixed in the vehicle: the roll axis is replaced by an x axis parallel to the ground, and the z axis passes downward through the center of mass of the vehicle. The suspension springs, dampers and active anti-roll bars generate moments between the sprung and unsprung masses in response to roll motions. The active roll control systems at each axle consist of a pair of actuators and a series of mechanical linkages in addition to the existing passive springs and dampers. The tires produce lateral forces that vary linearly with the side slip angles.

$$mv(\dot{\beta}+\dot{\psi}) - m_s h\ddot{\phi} = F_{yf} + F_{yr}, \tag{2.68}$$

$$-I_{xz}\ddot{\phi} + I_{zz}\ddot{\psi} = F_{yf}l_f - F_{yr}l_r + l_w \Delta F_b, \tag{2.69}$$

$$\begin{aligned}(I_{xx} + m_s h^2)\ddot{\phi} - I_{xz}\ddot{\psi} &= m_s g h\phi + m_s v h(\dot{\beta}+\dot{\psi}) - \\ -k_{f(r)}(\phi - \phi_{t,f}) - b_{f(r)}(\dot{\phi} - \dot{\phi}_{t,f}) &- k_{r(r)}(\phi - \phi_{t,r}) - b_{r(r)}(\dot{\phi} - \dot{\phi}_{t,r}),\end{aligned} \tag{2.70}$$

$$\begin{aligned}-rF_{yf} &= m_{uf} v(r - h_{uf})(\dot{\beta}+\dot{\psi}) + m_{uf} g h_{uf}\phi_{t,f} - \\ -k_{t,f(r)}\phi_{t,f} + k_{f(r)}(\phi - \phi_{t,f}) &+ b_{f(r)}(\dot{\phi} - \dot{\phi}_{t,f}),\end{aligned} \tag{2.71}$$

$$\begin{aligned}-rF_{yr} &= m_{ur} v(r - h_{ur})(\dot{\beta}+\dot{\psi}) - m_{ur} g h_{ur}\phi_{t,r} - \\ -k_{t,r(r)}\phi_{t,r} + k_{r(r)}(\phi - \phi_{t,r}) &+ b_{r(r)}(\dot{\phi} - \dot{\phi}_{t,r}).\end{aligned} \tag{2.72}$$

The lateral tire forces F_{yf} and F_{yr} in the direction of the wheel ground contact are approximated linearly to the tire slide slip angles α_f and α_r, respectively:

$$F_{yf} = \mu C_f \alpha_f, \quad F_{yr} = \mu C_r \alpha_r, \tag{2.73}$$

where μ is the side force coefficient (it is also called friction or cohesion co-efficient) and C_f and C_r are tire side slip constants. μ is also called friction or cohesion coefficient and by definition it is the ratio of the frictional force acting in the wheel plane and the wheel ground contact force.

The chassis and the wheels have identical velocities at the wheel ground contact points. The velocity equations for the front and rear wheels in the lateral and in the longitudinal directions are as follows:

$$v_{w,f}\sin(\delta_f - \alpha_f) = l_f \cdot \dot{\psi} + v\sin\beta \tag{2.74}$$

$$v_{w,f}\cos(\delta_f - \alpha_f) = v\cos\beta \tag{2.75}$$

$$v_{w,r}\sin\alpha_r = l_r \cdot \dot{\psi} - v\sin\beta \tag{2.76}$$

$$v_{w,r}\cos\alpha_r = v\cos\beta. \tag{2.77}$$

In stable driving conditions, the tire side slip angle α_i is normally not larger than 5° and the above equation can be simplified by substituting $\sin x \approx x$ and $\cos x \approx 1$. Thus, the classical equations for the tire side slip angles are then given as

$$\alpha_f = -\beta + \delta_f - \frac{l_f \cdot \dot{\psi}}{v}, \quad \alpha_r = -\beta + \frac{l_r \cdot \dot{\psi}}{v}. \tag{2.78}$$

By choosing the system states are the side slip angle of the sprung mass β, the yaw rate $\dot{\psi}$, the roll angle ϕ, the roll rate $\dot{\phi}$, the roll angle of the unsprung mass at the front axle $\phi_{t,f}$ and at the rear axle $\phi_{t,r}$, i.e.,

$$x = \left(\beta \;\; \dot{\psi} \;\; \phi \;\; \dot{\phi} \;\; \phi_{t,f} \;\; \phi_{t,r}\right)^T, \tag{2.79}$$

the differential algebraic model can be transformed into the following state space representation form:

$$E(v)\dot{x} = A_0(v)x + B_0\delta_f + B_1\Delta F_b \tag{2.80}$$

where $E(v)$ is an invertible matrix which also contains masses and inertias.

The system matrices are the following:

$$E(v) = \begin{bmatrix} mv & 0 & 0 & -m_s h & 0 & 0 \\ 0 & I_{zz} & 0 & -I_{xz} & 0 & 0 \\ -m_s vh & -I_{xz} & 0 & I_{xx} + m_s h^2 & -b_{f(r)} & -b_{r(r)} \\ -m_{uf} v(r - h_{uf}) & 0 & 0 & 0 & +b_{f(r)} & 0 \\ -m_{ur} v(r - h_{ur}) & 0 & 0 & 0 & 0 & +b_{r(r)} \\ 0 & 0 & 1 & 0 & 0 & 0 \end{bmatrix},$$

$$A_0(v) = \begin{bmatrix} -(C_f + C_r)\mu & \frac{(-l_f C_f + l_r C_r)\mu}{v} - mv & 0 & 0 & 0 & 0 \\ (-C_f l_f + C_r l_r)\mu & -\frac{(l_f^2 C_f + l_r^2 C_r)\mu}{v} & 0 & 0 & 0 & 0 \\ 0 & m_s vh & m_s gh - k_{f(r)} - k_{r(r)} & -b_{f(r)} - b_{r(r)} & k_{f(r)} & k_{r(r)} \\ -rC_f\mu & m_{uf} v(r - h_{uf}) - \frac{l_f r C_f \mu}{v} & k_{f(r)} & b_{f(r)} & A_{0(4,5)} & 0 \\ -rC_r\mu & m_{ur} v(r + h_{ur}) + \frac{l_r r C_r \mu}{v} & k_{r(r)} & b_{r(r)} & 0 & A_{0(5,6)} \\ 0 & 0 & 0 & 1 & 0 & 0 \end{bmatrix},$$

$$B_{10} = \begin{bmatrix} C_f\mu \\ l_f C_f \mu \\ 0 \\ rC_f\mu \\ 0 \\ 0 \end{bmatrix}, \quad B_{20} = \begin{bmatrix} 0 & 0 & 0 \\ 0 & 0 & l_w \\ 1 & 1 & 0 \\ 1 & 0 & 0 \\ 0 & 1 & 0 \\ 0 & 0 & 0 \end{bmatrix}.$$

using the notations $A_{0(4,5)} = -k_{t,f(r)} - k_{f(r)} + m_{uf} g h_{uf}$ and $A_{0(5,6)} = -k_{t,r(r)} - k_{r(r)} - m_{ur} g h_{ur}$.

By multiplying the left and right-hand sides of this equation by the $E^{-1}(v)$, the state space representation is yielded:

$$\dot{x} = A(v)x + B(v)\delta \tag{2.81}$$

where $\delta^T = \begin{bmatrix} \delta_f & \Delta F_b \end{bmatrix}$. If an active anti-roll bar system is also present, then one can introduce an additional control input $u_c = \begin{bmatrix} u_f & u_r \end{bmatrix}$ for the roll moments between the sprung and unsprung masses generated by the active anti-roll bars, i.e.,

$$\dot{x} = A(v)x + B(v)\delta + B_{rb}(v)u_c. \tag{2.82}$$

For the measured signals one can chose, e.g., the lateral acceleration, the yaw rate and the roll rate

$$y = \begin{bmatrix} a_y & \dot{\psi} & \dot{\phi} \end{bmatrix}^T, \tag{2.83}$$

where the lateral acceleration is $a_y = v\dot{\beta} + v\dot{\psi} - h\ddot{\phi}$.

Table 2.3 Parameters of the yaw–roll model

Params	Value
m_s	12,487 kg
m_{uf}, m_{ur}	706, 1000 kg
m	14,193 kg
h	1.15 m
$h_{uf} h_{ur}$	0.53, 0.53 m
r	0.83 m
C_f, C_r	$582 \cdot 10^3$ kN/rad, $783 \cdot 10^3$ kN/rad
k_f, k_r	$380 \cdot 10^3$ kNm/rad, $684 \cdot 10^3$ kNm/rad
b_f, b_r	$100 \cdot 10^3$ kN/rad, $100 \cdot 10^3$ kN/rad
$k_{t,f}, k_{t,f}$	$2060 \cdot 10^3$ kNm/rad, $3337 \cdot 10^3$ kNm/rad
I_{xx}	24,201 kg m^2
I_{xz}	4200 kg m^2
I_{zz}	34,917 kg m^2
l_f, l_r	1.95, 1.54 m
l_w	0.93 m
μ	1

In the linear yaw–roll models the forward velocity is considered a constant parameter. However, the forward velocity is an important stability parameter, so that it is considered to be a variable of the motion. Thus, the modelling of combined yaw and roll dynamics of road vehicles leads to a nonlinear model, since the Eq. (2.81) the the system matrices depend on the forward velocity of the vehicle and the side force coefficient nonlinearly.

The forward velocity is approximately equivalent to the velocity in the longitudinal direction while the side slip angle β is small. It can be assumed that the side slip angle is small under stable driving conditions. Hence the driving throttle is constant during a lateral manoeuvre and the forward velocity only depends on the brake forces. The forward velocity is assumed to be measured, however, the side force coefficient is usually not directly measured.

If v and μ are selected as scheduling variables, the differential equations of the combined yaw and roll motion are linear in the state variables:

$$\dot{x} = A(\rho)x + B_1(\rho)\delta_f + B_2(\rho)\Delta F_b \tag{2.84}$$

where

$$\begin{aligned} A(\rho) &= A_0 + \rho_1 A_1 + \rho_2 A_2 + \rho_3 A_3 + \rho_4 A_4 + \rho_5 A_5, \\ B_1(\rho) &= B_{10} + \rho_2 B_{11} + \rho_3 B_{12}, \\ B_2(\rho) &= B_{20} + \rho_1 B_{21}. \end{aligned}$$

where $\rho = [\rho_1\ \rho_2\ \rho_3\ \rho_4\ \rho_5]$ with $\rho_1 = \frac{1}{v}$, $\rho_2 = \mu$, $\rho_3 = \mu/v$, $\rho_4 = \mu/v^2$, $\rho_5 = v$.

Possible parameters for a nominal model that corresponds to a heavy-vehicle are included in Table 2.3.

2.6 Grey-Box Identification and Parameter Estimation

LPV models that are obtained by using first principle considerations are full with parameters whose values are not necessarily known a priori. Thus, a method is necessary in order to estimate these unknown parameters of the nominal model. In what follows we consider the (q)LPV systems, as a subclass of the input-affine nonlinear systems, that can be cast as:

$$\begin{aligned} \dot{x} &= A(p, \rho(t))x + B_u(p, \rho(t))u + B_\varphi(p)\varphi(\rho(t)), \\ y &= C(p, \rho(t))x, \end{aligned} \tag{2.85}$$

where p is a parameter vector, $\rho(t)$ is a known vector of time-varying scheduling parameters that eventually depends on measured outputs, i.e., $\rho(t) = \rho(y)$, and φ is a known, possibly nonlinear, function of its arguments.

The objective of our investigations is to compute the unknown parameter p for system (2.85) from input-output measurements, in other words, to solve a grey-box identification problem. A widely used idea to solve such an identification problem is to set a quadratic output error identification criterion, i.e., to minimize the problem as a function of the unknown parameter.

The objective function of this nonlinear least squares problem is usually given by

$$J(p) = \frac{1}{2}\|y - y(p)\|^2, \tag{2.86}$$

where $y(p)$ is the solution of (2.85) corresponding to input u and a suitable initial condition x_0. For practical reasons a norm induced by a discrete scalar product is used, e.g.,

$$\|v\|^2 := \frac{1}{N}\sum_{i=0}^{N-1} |v(t_i)|^2, \tag{2.87}$$

$v(t_i)$ being the samples of the signal v at the time instances t_i. In a practical identification experiment the sampling is uniform, the sampling time being τ, i.e., $t_i = t_0 + (i-1)\tau$. Usually, some additional box constrains

$$p_{i,l} \le p_i \le p_{i,u}, \quad i = 1, \cdots, n_p \tag{2.88}$$

on the parameter range are also available, permitting to set a constrained nonlinear least squares problem.

In a discrete-time setting there are several methods dedicated to the solution of this problem, see, e.g., Bamieh and Giarre (2002), Hori et al. (1992), Lee and Poola (1996, 1999), Ljung (2001), Verdult and Verhaegen (2002). In these approaches the optimization scheme in general is based on a Newton or quasi Newton type iteration process. Other methods, which are often termed as "adaptive" or "recursive", e.g., the Extended Kalman Filter (EKF) method, can be considered mainly as a recursive variant of these types of algorithms, where the main benefit, from an algorithmic point of view, is expected to be the low number of simulations needed. The general convergence properties of these type of methods, even in a theoretical setting, are little known.

In the continuous-time setting one can also apply these type of methods, all of them involving the integration of a system of type (2.85). This integration poses some problems that are new or are more stringent than the difficulties encountered in the discrete-time case.

The first problem is caused by the fact that the initial condition x_0 is often unknown in a practical setting. Besides the general theoretical question of identifiability one has to cope with the problem that in order to evaluate the functional (2.86), one has to integrate the system that contains the parameter p starting from the same initial condition as the original one. In a discrete time setting, at least in the case when sufficiently long data record is available, this problem can be solved by starting the simulation from a shifted initial time and by using the previous data as an initial condition. In order to overcome this difficulty we propose to set a modified identification problem. We propose to design a so called Luenberger type observer first, and then to perform the identification process for the observer system.

The simulation process, i.e., the method that computes $y(p, t_i)$, consists of a numerical algorithm, which performs an implicit discretization of the system. For a certain class of differential equations, i.e., stiff equations, these numerical methods are quite involved, containing implicit schemes with variable step length iterations. A closer analysis of this fact implies one of the inherent difficulties in the continuous-time parameter identification process.

To highlight the problem, note that in order to compute the solution with acceptable accuracy, the integration scheme needs the evaluation of the right hand of the differential equation in an intermediate time instance t, i.e., at $t_i \leq t \leq t_{i+1}$. The problem is, that values $\rho(t)$, $u(t)$ and $y(t)$, are not available during the simulation

process and they have to be replaced somehow, e.g., by interpolation or by a zero order hold strategy. Thus the quantization of the input u and of the scheduling variables ρ results in a modified differential equation. The solution of this equation might differ considerably from that of the original one.

2.6.1 Observer-Based Identification

If the system (2.85) is started from different initial states $\hat{x}_0$, the corresponding solution $\hat{y}$ will differ, in general, from the solution y. Moreover, for a nonlinear system this error is not an additive term with exponentially decay. It follows, that the objective functional will not vanish for the solution of the system determined by the nominal parameter p. Thus the applied optimization algorithms will fail to provide the correct parameter value.

If the initial condition x_0 is unknown, one has to extend the states of the original system with the unknown parameters, and add $\dot{p} = 0$ to the set of state equations. Observability of this extended system guarantees the uniqueness of the solution function corresponding to the pair $(p, x_0(p))$. However, the extended system is usually a full nonlinear system whose observability is hard to be tested in practice. In what follows it is assumed that identifiability under the condition of unknown initial condition holds.

In order to cope with the problem of unknown initial conditions, we propose to design a Luenberger type observer for the system, and then to perform the identification process for the observer system. The form of the observer is the following:

$$\begin{aligned}\dot{\eta} =&(A + KC)(\rho, p)\eta + (B_u + KD)(\rho, p)u + B_\varphi(\rho, p)\varphi - K(\rho, p)y\\ \varepsilon =& - C(\rho, p)\eta + y.\end{aligned} \tag{2.89}$$

By construction, for $p = p_0$ system (2.89) is an observer, i.e., for the nominal value of the parameters one has $\lim_{t\to\infty} \varepsilon(t) = 0$. That means that in practice the objective function (2.86) can be replaced by the function

$$\tilde{J}(p) = \frac{1}{2}\langle \varepsilon, \varepsilon\rangle_o, \quad \langle \varepsilon, \varepsilon\rangle_o := \frac{1}{N-L}\sum_{i=L}^{N-1} |\varepsilon(t_i)|^2, \tag{2.90}$$

with a properly chosen thread L. The choice of the thread depends on the convergence properties (time constants), of the observer, i.e., from the choice of observer gain K.

Concerning the question of stability, let us recall, that an LPV system is said to be quadratically stable if there exist a matrix $P = P^T > 0$ such that

$$A(\rho)^T P + PA(\rho) < 0 \tag{2.91}$$

for all the parameters $\rho \in \mathscr{P}$. A necessary and sufficient condition for a system to be quadratically stable is that the condition in Eq. (2.91) holds for all the corner points of the parameter space, i.e., one can obtain a finite system of LMI's that has to be fulfilled for $A(\rho)$ with a suitable positive definite matrix P, see Gahinet and Apkarian (1996), Fen et al. (1996).

In order to obtain a quadratically stable observer the LMI:

$$(A(\rho) + K(\rho)C)^T P + P(A(\rho) + K(\rho)C) < 0 \tag{2.92}$$

must hold for suitable $K(\rho)$ and $P = P^T > 0$. By introducing the auxiliary variable $G(\rho) = PK(\rho)$, one has to solve the following set of LMIs on the corner points of the parameter space:

$$A(\rho)^T P + PA(\rho) + C^T G(\rho)^T + G(\rho)C < 0 \tag{2.93}$$

By solving these LMIs one can obtain a suitable observer gain for a fixed, but arbitrary value of p.

2.6.2 Adaptive Observer-Based Approach

Adaptive observers are used mainly for fault detection and isolation and adaptive control purposes and they are meant to work on-line. In our identification setting the observer works off-line and it has to converge to acceptable values of the estimated parameters in the time given by the length of the measurements.

Our approach starts from the ideas from the general nonlinear theory, see Besancon (2000). It is assumed the existence of symmetric and positive definite matrix P, a gain matrix $K(t)$, a matrix M and $\mu > 0$ such that

$$PA_o(t) + A_o^T(t)P \leq -\mu I, \quad PB_p = C^T M, \tag{2.94}$$

where $A_o(t) = A(t) + K(t)C$ hold and that the signals φ are persistently exciting.

Then, the adaptive observer used for identification can be defined as:

$$\begin{aligned}\dot{\hat{x}} &= A(t)\hat{x} + B_u(t)u + B_p\varphi(t)\hat{p} + K(t)(y - C\hat{x})\\ \dot{\hat{p}} &= -\gamma\varphi^T(t)M^T(y - C\hat{x}),\end{aligned}$$

where M is assumed to meet conditions (2.94).

In an off-line identification setting the persistency condition

$$\int_t^{t+T} \varphi^T(\tau)B_p^T B_p\varphi(\tau)d\tau \geq \alpha I \tag{2.95}$$

is meant to be fulfilled in a finite time window determined by the measurement length and the value of T. The adaptive observer setting guarantees the exponential convergence rate. Knowing an estimation for this time constant one can determine the required measurement length in order to be able to estimate the parameters with sufficiently accuracy. Therefore an identification experiment is designed by considering these two factors, the persistency requirement and the desired convergence properties.

The performance properties of the observer depends heavily on the choice of the gain $K(t)$ and the parameter γ. By choosing γ properly, one can improve the convergence rate of the parameters. Further research is done in order to give a theoretically justified design procedure for these parameters.

Finding the unknown parameters requires the solution of certain differential equations, for an overview see Polak (1997). Although we embed the system in the class of (q)LPV systems, in general, we cannot exploit the linear structure in the solution process, and we have to use a general differential equation solver. For the observer design of the LTI system the effect of quantization is shown, e.g., in Sur and Paden (1998).

2.7 Parameter Estimation: Case Studies

2.7.1 Identification of a Suspension System

Model based suspension design relies on the knowledge of the physical parameters of the vehicle. For a given vehicle, however, these parameters are usually not known. Moreover the system is nonlinear and contains uncertain and time-varying components. Therefore the usual linear techniques are not suitable to handle this estimation problem. In what follows a nonlinear, quasi LPV (qLPV) model structure is used as a starting point for the identification. It is assumed that the accelerations of the sprung and unsprung masses and the relative displacement can be measured directly. For the complete identification of the model the knowledge of the road signal is indispensable.

Having found the identified model a method is presented for the reconstruction of the road disturbance. Due to the nonlinear nature of the model the unmeasured—but computable—relative velocity signal is also needed.

After the reconstruction of the road roughness signal one has a freedom in the choice of the post-processing method, which can be on-line or off-line and which aims to classify roads by their roughness. In the literature there are many papers with different approaches on the estimation of road roughness. The road surface can be examined as a stochastic process which can be estimated from a white noise source by using an appropriate transfer function Hac (1987), Sayers (1986).

The state space representation of the nonlinear model of a quarter car is written as:

$$\begin{bmatrix}\dot{x}_1\\ \dot{x}_2\\ \dot{x}_3\\ \dot{x}_4\end{bmatrix} = \begin{bmatrix} 0 & 0 & 1 & 0\\ 0 & 0 & 0 & 1\\ -\frac{k_s^l}{m_s} & \frac{k_s^l}{m_s} & \frac{b_s^l}{m_s} & \frac{b_s^l}{m_s}\\ \frac{k_s^l}{m_u} & -\frac{k_s^l}{m_u} - \frac{k_t}{m_u} & \frac{b_s^l}{m_u} & \frac{b_s^l}{m_u}\end{bmatrix}\begin{bmatrix}x_1\\ x_2\\ x_3\\ x_4\end{bmatrix} + \begin{bmatrix} 0 & 0 & 0\\ 0 & 0 & 0\\ \frac{k_s^{nl}}{m_s} & -\frac{b_s^{sym}}{m_s} & \frac{b_s^{nl}}{m_s}\\ -\frac{k_s^{nl}}{m_u} & \frac{b_s^{sym}}{m_u} & -\frac{b_s^{nl}}{m_u}\end{bmatrix}\begin{bmatrix}\rho_k^3\\ |\rho_b|\\ \sqrt{|\rho_b|}\,\mathrm{sgn}(\rho_b)\end{bmatrix} + \begin{bmatrix}0\\0\\0\\ \frac{k_t}{m_u}\end{bmatrix} w \tag{2.96}$$

where $\dot{x}_1 = x_3$ and $\dot{x}_2 = x_4$.

It is assumed that the accelerations $y_1 = \ddot{x}_1$ and $y_2 = \ddot{x}_2$ and the relative displacement $\rho_k = x_2 - x_1$ can be measured directly, and the relative velocity, i.e., $x_4 - x_3$ is then calculated with numerical integration from the measured signals. It is also assumed that the values for m_s and m_u are also known. Thus, in our case the relative velocity and the relative displacement can be selected as scheduling parameters:

$$\rho_b = x_4 - x_3 \quad \rho_k = x_2 - x_1 \tag{2.97}$$

Let us denote the column vector by $\phi(\rho_k, \rho_b)$

$$\phi(\rho_k, \rho_b) = \begin{bmatrix}\rho_k^3 & |\rho_b| & \sqrt{|\rho_b|}\,\mathrm{sgn}(\rho_b)\end{bmatrix}^T. \tag{2.98}$$

If one considers $\phi(\rho_k, \rho_b)$ as a fictitious input, then, the state space representation of the qLPV model is:

$$\dot{x} = \begin{bmatrix} 0 & 0 & 1 & 0\\ 0 & 0 & 0 & 1\\ -p_{11} & p_{11} & -p_{12} & p_{12}\\ p_{21} & -p_{21} - p_t & p_{22} & -p_{22}\end{bmatrix} x + \begin{bmatrix} 0 & 0 & 0\\ 0 & 0 & 0\\ p_{13} & -p_{14} & p_{15}\\ -p_{23} & p_{24} & -p_{25}\end{bmatrix}\phi(\rho_k, \rho_b) + \begin{bmatrix}0\\0\\0\\ p_t\end{bmatrix} w \tag{2.99}$$

where

$$\begin{bmatrix} p_{11} & p_{12} & p_{13} & p_{14} & p_{15}\\ p_{21} & p_{22} & p_{23} & p_{24} & p_{25}\end{bmatrix} = \begin{bmatrix} \frac{k_s^l}{m_s} & \frac{b_s^l}{m_s} & \frac{k_s^{nl}}{m_s} & \frac{b_s^{sym}}{m_s} & \frac{b_s^{nl}}{m_s}\\ \frac{k_s^l}{m_u} & \frac{b_s^l}{m_u} & \frac{k_s^{nl}}{m_u} & \frac{b_s^{sym}}{m_u} & \frac{b_s^{nl}}{m_u}\end{bmatrix} \tag{2.100}$$

$$p_t = \frac{k_t}{m_u} \tag{2.101}$$

Let us use the following formulae: $v(x_2, w) = p_t(x_2 - w)$, $\gamma = m_u/m_s$. From Eq. (2.99) follows, that

$$\gamma y_1 + y_2 = -v(x_2, w), \tag{2.102}$$

where

$$y_1 = p_{11}\rho_k + p_{12}\rho_b + [p_{13} \quad -p_{14} \quad p_{15}]\phi(\rho_k, \rho_b).$$

If one can determine ρ_b then the values of the parameters can be determined from Eq. (2.99) by using a least squares (LS) estimation. The values of ρ_b are estimated by using a second order scheme,

$$\dot{y}(t) = \frac{y(t + \Delta) - y(t)}{\Delta} - \frac{\Delta}{2}\ddot{y}(t),$$

i.e.,

$$\rho_b(t) = \frac{\rho_k(t + \Delta) - \rho_k(t)}{\Delta} - \frac{\Delta}{2}(y_2(t) - y_1(t)), \tag{2.103}$$

where Δ is the sampling time. To determine the value of p_t from Eq. (2.102), the value of the unsprung mass displacement x_2 is needed. Combining (2.99) and (2.102) after a simulation step x_2 can be obtained and then a value for p_t is yielded by carrying out an LS estimation. The signal x_2 can also be determined from the equation

$$\ddot{x}_2 = -p_{21}\rho_k - p_{22}\rho_b + [-p_{23}, p_{24}, -p_{25}]\phi(\rho_k, \rho_b) - \gamma y_1 - y_2, \tag{2.104}$$

by using two consecutive integration steps.

If there are no on board excitations the signal representing the effect of the road surface on the suspension system can be detected by using Eq. (2.102) as:

$$w = \frac{\gamma y_1 + y_2}{p_t} + x_2. \tag{2.105}$$

If the value of p_t for the qLPV model of the quarter car suspension system is known and the unsprung mass displacement x_2 can be determined, then the road signal w can be determined. The value of x_2 is computed by integrating the system (2.104). Due to the effect of the unknown initial value in the reconstructed road signal $\hat{w}$ there is a systematic error present in the form of a linear trend.

In order to classify different roads Hac (1987) has proposed a parameter based method. In this paper a slight modification of this model is used where the road signal is given by the following continuous time model:

$$\dddot{w} + (a_1 + a_3)\ddot{w} + (a_0 + a_1a_3)\dot{w} + a_0a_1w = \xi \tag{2.106}$$

where ξ is a white noise process and parameters a_1, a_2, a_3 depend on the forward velocity and the road type, given as follows:

$$a_0 = (\alpha_2^2 + \beta^2)^2 v^2 + 4\alpha_2^2 \beta^2 v^4, \quad a_1 = \alpha_1 v,$$
$$a_2 = 2(\alpha_2^2 - \beta^2)v^2, \quad a_3 = (a_2 + 2a_0)^{1/2}.$$

For example for a paved road the values of these parameters are defined by $\alpha_1 = 0.5$, $\alpha_2 = 0.2$ and $\beta = 2.0$.

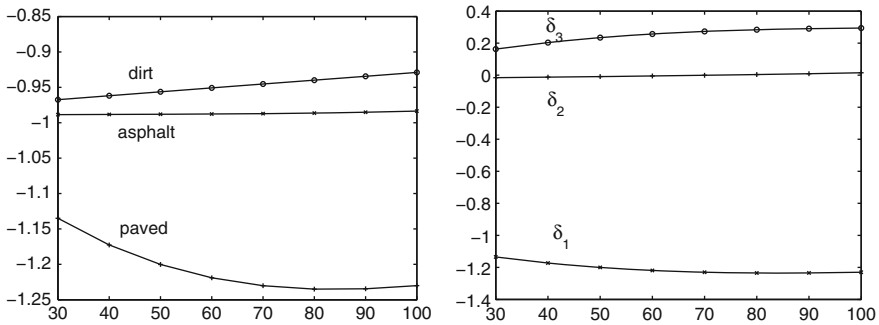
In an identification setting the continuous time modelling is not suitable, hence the road characteristics should be given in terms of the parameters of a discrete time model set:

$$\omega_t + \delta_1 \omega_{t-1} + \delta_2 \omega_{t-2} + \delta_3 \omega_{t-3} = \xi_t \tag{2.107}$$

These parameters also depend on the velocity and the road type. In Fig. 2.12a this dependence is depicted in case of an asphalt road for the parameters δ_1, δ_2 and δ_3, respectively. Figure 2.12b also shows parameter δ_1 in the function of the velocity. Using these type of figures the task of the classification of the road can be performed by estimating coefficients δ_i if the value of the velocity is known.

The approach presented above gives a global characterization of roads by using a basic statistical identification process. In this case the aim of the road parameter estimation is to give a classification of a longer road segment. If local information about road quality is needed other methods should be used, e.g., wavelet based techniques, for details see Gáspár et al. (2003a).

In the first example the accelerations $y_1 = \ddot{x}_1$, $y_2 = \ddot{x}_2$, the relative displacement $\rho_k = x_2 - x_1$ and the road signal w are given from the simulated model described by the nominal parameters:



(a) δ_1 (b) paved road

Fig. 2.12 Values of parameters for different road conditions

Table 2.4 Reconstructed values of p

p	57.97	2.41	0.68	0.34	810.34	284.94	11.86	3.38	1.69	3983.1
$p_{0.001}$	57.97	2.41	0.68	0.34	810.65	284.95	11.85	3.38	1.70	3984.6
$r_{0.001}$	0	0	0	0	0.04	0	0.08	0	0.59	0.04
$p_{0.005}$	58.11	2.37	0.69	0.37	797.03	285.62	11.69	3.43	1.82	3917.6
$r_{0.005}$	0.24	1.66	1.47	8.82	1.64	0.24	1.43	1.48	7.69	1.64
$p_{0.01}$	58.39	2.38	0.70	0.36	755.6933	287.02	11.70	3.44	1.79	3714.4
$r_{0.01}$	0.72	1.24	2.94	5.88	6.74	0.73	1.35	1.78	5.92	6.75

Table 2.5 Reconstructed values of p_t

p_t	$p_{t,0.001}$	$p_{t,0.005}$	$p_{t,0.01}$
3220.3	3284.3	3363.1	2723.3
r_t	1.98	4.43	15.43

$$p = \begin{pmatrix} 57.97 & 2.41 & 0.68 & 0.34 & 810.34 \\ 284.94 & 11.86 & 3.38 & 1.69 & 3983.1 \end{pmatrix}.$$

The values for the masses are $m_u = 59$ kg and $m_s = 290$ kg. Different sampling times Δ are used in the simulation. The results of the identification are given in p_Δ and $p_{t,\Delta}$ and are summarized in Table 2.4 and Table 2.5, where r_Δ denotes the relative error.

The relative error of the estimation of $p_1 \ldots p_5$ is below 7 % and the estimation of p_t is below 16 % when the sampling time is selected $\Delta = 0.01$ sec. If we select smaller sampling time ($\Delta = 0.005$ s) the relative error is below 5 %. If the sampling time is $\Delta = 0.001$ s the relative error is below 2 %. The appropriate selection of the sampling time is significant in the sufficient estimation, however, the practice influences this selection.

As far as the road signal reconstruction is concerned the value of the estimate of p_t is decisive. The results show the importance of the choice of the sampling time. An estimation for the sampling time needed can be carried out by the Shannon theorem, which is only applied to the linear part of the model used in the identification process, i.e.,

$$\begin{bmatrix} 0 & 0 & 1 & 0 \\ 0 & 0 & 0 & 1 \\ -p_{11} & p_{11} & -p_{12} & p_{12} \\ p_{21} & -p_{21} & p_{22} & -p_{22} \end{bmatrix}.$$

Figure 2.13 shows the effect of the sampling time on the reconstruction of the unsprung mass displacement x_2, which also plays a central role in the reconstruction of the road signal.

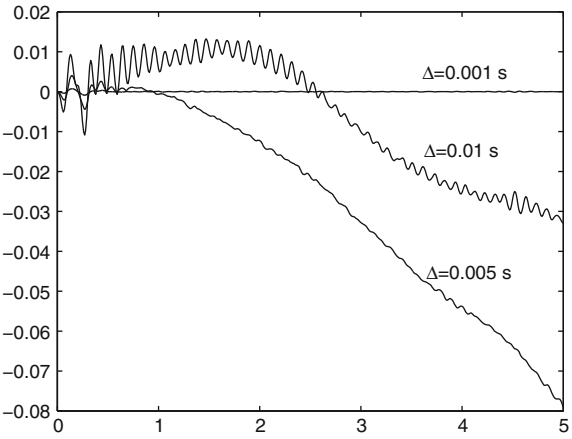


Fig. 2.13 Absolute errors for x_2 corresponding to different sampling times

Table 2.6 Identification results

v	Parameter	δ_1	δ_2	δ_3
40	Nominal	−0.988	−0.007151	0.00213
	Identified	−0.9878	0.007174	0.001743
60	Nominal	−0.9882	−0.006968	0.00618
	Identified	−0.9881	−0.006993	0.005798
80	Nominal	−0.9858	−0.007205	0.008486
	Identified	−0.9878	−0.007242	0.009956

In the second demonstration example three situations, which corresponds to an asphalt road and to different travelling velocities were simulated. The sampling time was set at 0.001 s. After reconstructing the road signal, the parameters δ_i of the discrete model (2.107) were estimated. The results are shown in Table 2.6.

2.7.2 Identification of the Yaw–Roll System

In rollover prevention methods in which the control design is based on the modelling of yaw–roll dynamics, the estimation of the CG is very important. In this section an estimation procedure for the position and height of the center of gravity (CG) is illustrated through a demonstration example. The real problem is that the physical model is of nonlinear continuous-time and the unknown parameter must be estimated by using a grey-box identification method. As a consequence of nonlinearity, the other difficulty is that the selection or estimation of the initial conditions is critical.

Figure 2.11 illustrates the combined yaw–roll dynamics of a vehicle. Recall that the qLPV model can be transformed into a state space representation form

$$\dot{x} = A(v)x + B(v)\delta, \quad x = \begin{bmatrix}\beta & \dot{\psi} & \phi & \dot{\phi} & \phi_{t,f} & \phi_{t,r}\end{bmatrix}^T, \quad \delta^T = \begin{bmatrix}\delta_f & \delta_b\end{bmatrix}$$

with $A(v) = E^{-1}A_0(v)$, $B_v = E^{-1}\begin{bmatrix}B_0 & B_1\end{bmatrix}$, where

$$E(v) = \begin{bmatrix} mv & 0 & 0 & -m_s h & 0 & 0 \\ 0 & I_{zz} & 0 & -I_{xz} & 0 & 0 \\ -m_s vh & -I_{xz} & 0 & I_{xx} + m_s h^2 & -b_f & -b_r \\ m_f v(r - h_f) & 0 & 0 & 0 & -b_f & 0 \\ m_r v(r - h_r) & 0 & 0 & 0 & 0 & -b_r \\ 0 & 0 & 1 & 0 & 0 & 0 \end{bmatrix},$$

$$A_0(v) = \begin{bmatrix} Y_\beta & Y_{\dot{\psi}} - mv & 0 & 0 & 0 & 0 \\ N_\beta & N_{\dot{\psi}} & 0 & 0 & 0 & 0 \\ 0 & m_s hv & a_{33} & -b_f - b_r & k_f & k_r \\ -rY_\beta & rY_f - m_f vh_f & -k_f & -b_f & k_{tf} & 0 \\ -rY_\beta & -rY_r - m_r vh_r & -k_r & -b_r & 0 & k_{tr} \\ 0 & 0 & 0 & 1 & 0 & 0 \end{bmatrix}$$

$$B_0 = \begin{bmatrix}Y_\delta & N_\delta & 0 & rY_\delta & 0 & 0\end{bmatrix}^T,$$

$$B_1 = \begin{bmatrix} -\delta_f & -d_1 - d_2\delta_f & 0 & 0 & 0 & 0 \\ -\delta_f & d_1 - d_2\delta_f & 0 & 0 & 0 & 0 \\ 0 & -\frac{l_w}{2} & 0 & 0 & 0 & 0 \\ 0 & \frac{l_w}{2} & 0 & 0 & 0 & 0 \end{bmatrix}^T.$$

The measured signals are the lateral acceleration, the yaw rate and the roll rate, i.e.,

$$y = \begin{bmatrix}a_y & \dot{\psi} & \dot{\phi}\end{bmatrix}^T, \tag{2.108}$$

where the lateral acceleration is $a_y = v\dot{\beta} + v\dot{\psi} - h\ddot{\phi}$. In the identification context the measuring of the roll rate seems to be obvious, since the parameter CG affects the roll dynamics rather than other dynamics: $y = \dot{\phi}$. The unknown parameters are the sprung mass m_s and the height h of CG. The real values of these parameters used in the simulation are $m_s = 12.48$ and $h = 1.15$.

The system does not depend affinely from the unknown parameters. Therefore it was necessary to manipulate the original system equations in order to obtain systems that might be useful from an identification point of view. Introducing the new variable $\zeta = I_{zz}\dot{\psi} - I_{xz}\dot{\phi}$ and considering the unknown parameter $\nu = 1/(m - m_s)$ one can obtain the system

$$\dot{x}_1 = A_{s,1}(\nu, v)x_1 + B_{s,1}(\nu, v)w \tag{2.109}$$

where $x_1 = \begin{bmatrix}\beta & \zeta\end{bmatrix}^T$ and $w = \begin{bmatrix}\delta_f & \delta_{b,r} & \dot{\psi} & \dot{\phi} & a_y\end{bmatrix}^T$. The matrices in (2.109) are the following:

$$A_{s,1}(v, v) = \begin{bmatrix} v\frac{Y_\beta}{v} & 0 \\ N_\beta & \frac{N_{\dot{\psi}}}{I_{zz}} \end{bmatrix}$$

$$B_{s,1}(v, v) = \begin{bmatrix} v\frac{Y_\delta}{v} & 0 & v\frac{Y_{\dot{\psi}}}{v} - 1 & 0 & -v\frac{m}{v} + \frac{1}{v} \\ N_\delta & -\frac{l_w}{2} & 0 & I_{xz}\frac{N_{\dot{\psi}}}{I_{zz}} & 0 \end{bmatrix}$$

Considering the unknown parameter $\alpha = m_s h$ one can write the equations

$$\dot{x} = A_{s,2}(v)x + B_{s,2}(v)\delta + \alpha B_{a,2}(v)\omega \tag{2.110}$$

where $A_{s,2} = E_2^{-1}A_2$, $B_{s,2} = E_2^{-1}B_s$ and $B_{a,2} = E_2^{-1}B_a$ with

$$E_2(v) = \begin{bmatrix} mv & 0 & 0 & 0 & 0 & 0 \\ 0 & I_{zz} & 0 & -I_{xz} & 0 & 0 \\ 0 & -I_{xz} & 0 & I_{xx} & -b_f & -b_r \\ m_f v(r - h_f) & 0 & 0 & 0 & -b_f & 0 \\ m_r v(r - h_r) & 0 & 0 & 0 & 0 & -b_r \\ 0 & 0 & 1 & 0 & 0 & 0 \end{bmatrix},$$

$$A_2(v) = \begin{bmatrix} Y_\beta & Y_{\dot{\psi}} - mv & 0 & 0 & 0 & 0 \\ N_\beta & N_{\dot{\psi}} & 0 & 0 & 0 & 0 \\ 0 & 0 & -k_f - k_r & -b_f - b_r & k_f & k_r \\ -rY_\beta & rY_f - m_f v h_f & -k_f & -b_f & k_{tf} & 0 \\ -rY_\beta & -rY_r - m_r v h_r & -k_r & -b_r & 0 & k_{tr} \\ 0 & 0 & 0 & 1 & 0 & 0 \end{bmatrix}$$

$$B_a = \begin{bmatrix} 0 & 0 & g & 0 & 0 & 0 \\ 1 & 0 & 0 & 0 & 0 & 0 \\ 0 & 0 & 1 & 0 & 0 & 0 \end{bmatrix}^T, \quad B_s = \begin{bmatrix} B_0 & B_1 \end{bmatrix}^T,$$

and $\omega = \begin{bmatrix}\phi & \ddot{\phi} & a_y\end{bmatrix}^T$.

Thus we obtain two qLPV systems that depend affinely on the unknown parameters, however, the expressions that corresponds to φ in (2.85) also contain unmeasured signals. It is difficult and yet unsolved problem to construct an adaptive observer in this general case. Therefore an estimation for the unmeasured signals β, ϕ and $\ddot{\phi}$ is needed. The signal ϕ is obtained by integrating the measured signal $\dot{\phi}$. The unknown integration constant $\phi(0)$ is introduced as an additional parameter that must be determined. For simplicity in our simulation example this value is set to zero.

The signal β is estimated from the equation

$$\dot{\zeta} = \frac{N_{\dot{\psi}}}{I_{zz}}\zeta + N_\beta\beta + \begin{bmatrix} N_\delta & -\frac{l_w}{2} & 0 & I_{xz}\frac{N_{\dot{\psi}}}{I_{zz}} & 0 \end{bmatrix} w, \tag{2.111}$$

where $\dot{\zeta}$ is estimated from ζ from a finite difference scheme. The signal $\ddot{\phi}$ is also estimated from $\dot{\phi}$ with another finite difference scheme.

The accuracy of the estimation of β is improved by using an unknown input estimation algorithm starting from (2.111):

$$\dot{\hat{\zeta}} = \frac{N_{\dot{\psi}}}{I_{zz}}\hat{\zeta} + N_\beta\hat{\beta} + \left[N_\delta \; -\tfrac{l_w}{2} \; 0 \; I_{xz}\tfrac{N_{\dot{\psi}}}{I_{zz}} \; 0\right]w - k(\hat{\zeta} - \zeta), \tag{2.112}$$

$$\hat{\beta} = \beta_0 - \delta(\hat{\zeta} - \zeta), \tag{2.113}$$

where β_0 is our initial estimate, for details. In our example the values $\delta = 500$ and $k = 700$ are used.

In order to fulfil the condition about persistent excitedness, the identification method is based on signals collected during in a cornering manoeuvre. The cornering manoeuvre starts at 1 s The steering angle applied in the simulation is a ramp signal. It reaches the maximum value in 0.5 s and filtered at 4 rad/s to represent the finite bandwidth of the driver. In the simulation experiment the forward velocity of the heavy vehicle varies between 40 and 65 km h due to a braking force. Two sampling times are applied, i.e., $T_{s1} = 0.01$ s, and $T_{s2} = 0.001$ s. The input and measured output signals are depicted in Fig. 2.14. The results of the identification are summarized in Table 2.7.

Figure 2.15 shows the convergence of the estimated parameters in our experiment for the given sampling times. As it is expected the convergence is smoother and quicker when the sampling time is smaller. However in practical applications the highest value of the sampling time, i.e., $T_s = 0.01$ s is used and the results show that this value is still acceptable in order to maintain a required accuracy of the estimated parameters.

In what follows we will use the notations of Sect. 2.5.3 and those of Fig. 2.11. Recall that the model equations can be expressed in a state space representation by considering the state vector:

$$x = \left[\beta \; \dot{\psi} \; \phi \; \dot{\phi} \; \phi_{t,f} \; \phi_{t,r}\right]^T \tag{2.114}$$

as

$$\dot{x} = A(\rho)x + B(\rho)u, \tag{2.115}$$

with

$$A(\rho) = A_0 + \rho_1 A_1 + \rho_2 A_2 + \rho_3 A_3, \quad B(\rho) = B_0 + \rho_1 B_1 + \rho_2 B_2 + \rho_4 B_4,$$

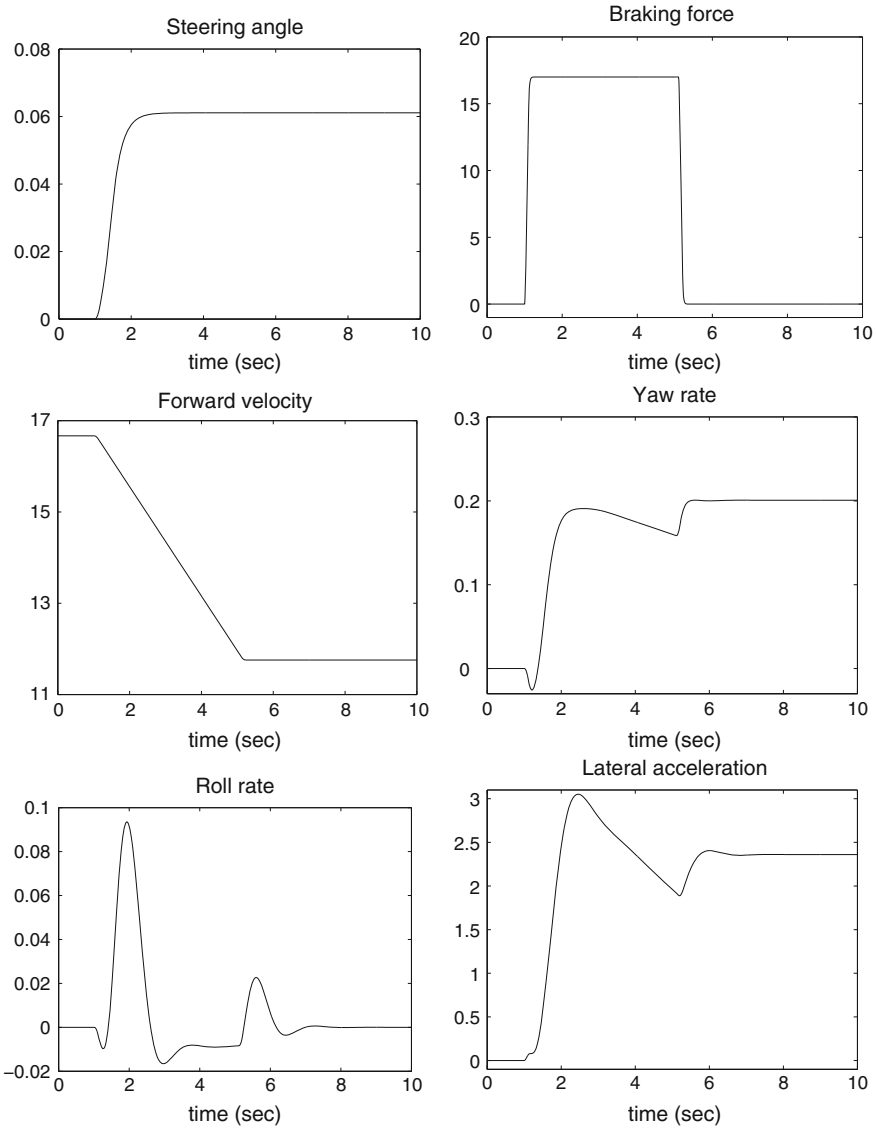


Fig. 2.14 Signals in the simulation example

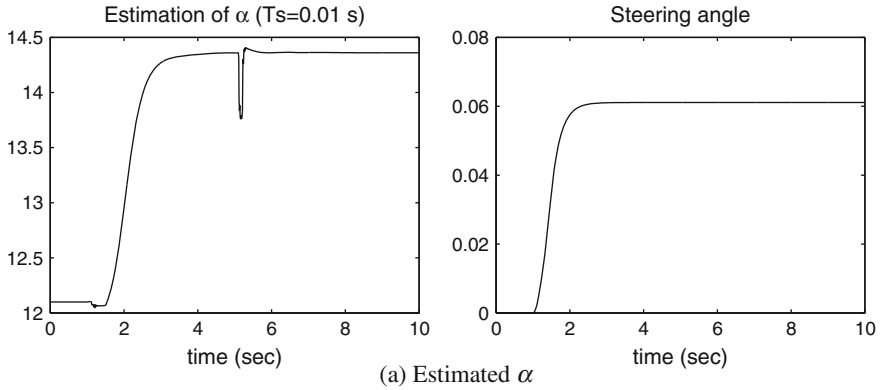
where the components of the scheduling vector ρ are

$$\rho_1 = \mu, \quad \rho_2 = \frac{\mu}{v}, \quad \rho_3 = \frac{\mu}{v^2}, \quad \rho_4 = \frac{1}{v}.$$

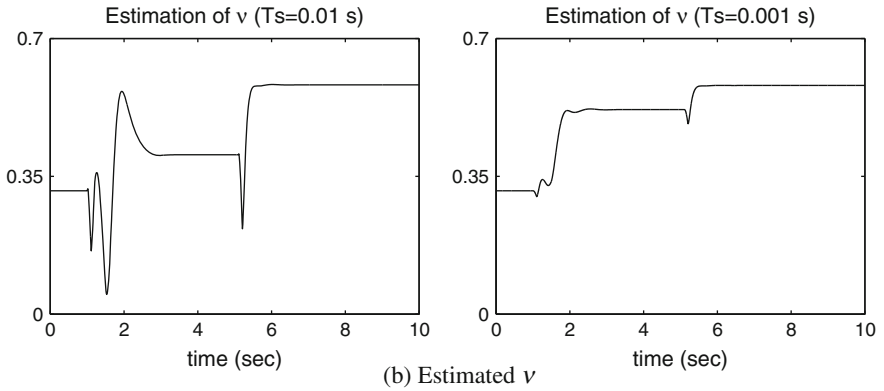
Table 2.7 Results of the identification

T_s	$\hat{\alpha}$	$\hat{\nu}$	$\hat{m}_s$	$\hat{h}$
0.01	0.5807	14.3601	12.4709	1.1515
0.001	0.5822	14.3601	12.4754	1.1511

The real values: $m_s = 12.487$ and $h = 1.15$



(a) Estimated α



(b) Estimated ν

Fig. 2.15 Estimated parameters

The components of the state matrices are the following:

$$A_0 = \begin{bmatrix} 0 & -1 \\ 0 & 0 \end{bmatrix}, \qquad A_1 = \begin{bmatrix} 0 & 0 \\ \frac{(C_f+C_r)I_{xz}}{(m_s-m)hI_{zz}} & \frac{C_r l_r^2 - C_f l_f^2}{I_{zz}} \end{bmatrix},$$

$$A_2 = \begin{bmatrix} \frac{C_f+C_r}{m_s-m} & 0 \\ \frac{C_r l_r - C_f l_f}{I_{zz}} & \frac{(C_r l_r - C_f l_f)I_{xz}}{(m-m_s)hI_{zz}} \end{bmatrix}, \quad A_3 = \begin{bmatrix} 0 & \frac{C_r l_r - C_f l_f}{m-m_s} \\ 0 & 0 \end{bmatrix},$$

$$B_0 = \begin{bmatrix} 0 & 0 & 0 \\ \frac{m_s I_{xz}}{(m_s - m)h I_{zz}} & 0 & \frac{l_w}{I_{zz}} \end{bmatrix}, \qquad B_1 = \begin{bmatrix} 0 & 0 & 0 \\ 0 & \frac{C_f}{(m-m_s)h} & \frac{I_{xz}}{I_{zz}} + \frac{C_f l_f}{I_{zz}} & 0 \end{bmatrix},$$

$$B_2 = \begin{bmatrix} 0 & \frac{C_f}{m-m_s} & 0 \\ 0 & 0 & 0 \end{bmatrix}, \qquad B_4 = \begin{bmatrix} \frac{m}{m-m_s} & 0 & 0 \\ 0 & 0 & 0 \end{bmatrix}.$$

The measured signals are the lateral acceleration $a_y = v\dot{\beta} + v\dot{\psi} - h\ddot{\phi}$, the roll rate and the yaw rate while the control input signals are the steering angle and the difference in the brake forces. Later the lateral acceleration is also selected as a fictitious input. It is also assumed that the forward velocity is available.

The estimation of the unknown parameters in the model is based on the equations of the lateral and the yaw dynamics of the vehicle, see Eqs. (2.68) and (2.69). Since β and $\dot{\beta}$ are unknown and not measured, a direct estimation algorithm cannot be applied. Thus, it is necessary to manipulate the original system equations in order to obtain systems that might be useful from an estimation point of view.

Observe first, that the lateral acceleration is a measured signal, which has direct relation to $\dot{\beta}$. By eliminating both β and $\dot{\beta}$ we get

$$a_1\ddot{\phi} + a_2\ddot{\psi} = \mu(a_3\dot{\psi} + a_4\delta_f) + (a_5 a_y + a_6 \Delta F_b), \tag{2.116}$$

where

$$\begin{aligned} a_1 &= (m - m_s)h(l_r C_r - l_f C_f) - I_{xz}(C_f + C_r), \\ a_2 &= I_{zz}(C_f + C_r), \\ a_3 &= -\frac{1}{v} C_f C_r l^2, \\ a_4 &= C_f C_r l, \\ a_5 &= -m(l_r C_r - l_f C_f) \\ a_6 &= l_w(C_f + C_r). \end{aligned}$$

Equation (2.116) is transformed in the following form:

$$\dot{v} = \mu u_1 + u_2, \tag{2.117}$$

where

$$\begin{aligned} v &= a_1\dot{\phi} + a_2\dot{\psi}, \\ u_1 &= a_3\dot{\psi} + a_4\delta_f, \\ u_2 &= a_5 a_y + a_6 \Delta F_b. \end{aligned}$$

Assuming that the signals $\dot{\psi}$, $\dot{\phi}$, a_y, δ_f, ΔF_b, v are measured or calculated, the values of v, u_1, u_2 can be computed. Since the values $\dot{v}$ are not available, the least

squares (LS) method cannot be applied directly in this problem. Next, a possible method is proposed for the estimation of the parameter μ from the Eq. (2.117) where v, u_1, and u_2 are known.

Both sides of (2.117) are multiplied by $e^{\alpha t}$ and then an partial integration is performed. Using the partial integral form $v(t)$ can be expressed in the following way:

$$\begin{aligned} v(t) =& e^{-\alpha t} v(0) + \alpha e^{-\alpha t} \int_0^t e^{\alpha \tau} v(\tau) d\tau + \\ &+ \mu e^{-\alpha t} \int_0^t e^{\alpha \tau} u_1(\tau) d\tau + e^{-\alpha t} \int_0^t e^{\alpha \tau} u_2(\tau) d\tau. \end{aligned} \tag{2.118}$$

It is known that the solution of the system

$$\dot{w}(t) = -\alpha w(t) + v(t) \tag{2.119}$$

is $w(t) = e^{-\alpha t} w(0) + e^{-\alpha t} \int_0^t e^{\alpha \tau} v(\tau) d\tau$. Selecting $w = 0$ the filtered output of the system (2.119) is $v^f(t) = e^{-\alpha t} \int_0^t e^{\alpha \tau} v(\tau) d\tau$. Then the following relation is formulated:

$$\mu u_1^f(t) = v(t) - e^{-\alpha t} v(0) - \alpha v^f(t) - u_2^f(t), \tag{2.120}$$

where v^f, u_1^f, u_2^f are the filtered outputs of the systems with inputs v, u_1, u_2, respectively. Based on Eq. (2.120) one can construct different practical algorithms for the estimation of μ. Note that the choice $\alpha = 0$ corresponds to the case of the simple integration.

The equation, which is the basis of the identification, is the following:

$$\ddot{\psi} = \alpha_1 \ddot{\phi} + \alpha_2 u_f + \alpha_3 a_y + \alpha_4 \Delta F_b, \tag{2.121}$$

where the fictitious signal is $u_f = \delta_f - \frac{l}{v} \dot{\psi}$ and $\alpha_1 = -\frac{a_1}{a_2}$, $\alpha_2 = \mu \frac{a_4}{a_2}$, $\alpha_3 = \frac{a_5}{a_2}$, $\alpha_4 = \frac{a_6}{a_2}$.

Note, that the model which is applied both for the parameter estimation and the control design does not contain the adhesion coefficient, however it contains the multiplication of the tire side slip constant and the adhesion coefficient, $\tilde{C}_f = \mu C_f$ and $\tilde{C}_r = \mu C_r$. Thus, instead of the adhesion coefficient, this multiplication will be estimated. Applying an identification method to (2.121), the coefficients α_i are estimated. These coefficients are related to the unknown parameters I_{zz}, I_{xz}, $\tilde{C}_f$ and $\tilde{C}_r$, thus they can be expressed from the estimated values:

$$I_{zz} = \frac{l_w}{\hat{\alpha}_4}, \tag{2.122}$$

$$I_{xz} = I_{zz}\left(\hat{\alpha}_1 - \frac{m - m_s}{m} h\hat{\alpha}_3\right), \tag{2.123}$$

$$\tilde{C}_f = \frac{I_{zz}\hat{\alpha}_2 m}{l_f m + I_{zz}\hat{\alpha}_3}, \tag{2.124}$$

$$\tilde{C}_r = \frac{I_{zz}\hat{\alpha}_2 m}{l_r m - \hat{\alpha}_3 I_{zz}}. \tag{2.125}$$

In what follows, for the sake of simplicity, it is assumed that the value for I_{xx} is known. Based on the method outlined in this section it is possible to estimate its value, too.

The model used in the estimation of the side slip angle contains the adhesion coefficient, which is a time varying signal. These signals cannot be estimated simultaneously since the observer-based method assumes that the parameters in the LPV model are known and the scheduling variables are available in the estimation of the side slip angle. Thus, a three-step estimation procedure which is illustrated in Fig. 2.16 might be needed. In the initialization step the unknown parameters are estimated from Eqs. (2.122) and (2.124). In practice it is usually enough to calculate them only when the vehicle has started and already covered a certain distance. The estimated values of the adhesion coefficient is the initialization of the adaptive algorithm $\tilde{C}_{f0}$ and $\tilde{C}_{r0}$. The other parameters, i.e., the inertias can be considered constant in a long time period. Thus, the model initialization is rarely performed, e.g., after a maintenance or periodically depending on the distance traveled.

In the second step an adaptive identification method is carried out for the estimation of the changes of the adhesion coefficient in $\tilde{C}_f$ and $\tilde{C}_r$ by an adaptive observer scheme designed using (2.117). The procedure requires the vehicle to perform a manoeuvre, e.g., there must be a nonzero steering angle or a nonzero yaw rate so that the signal u_1 is not identically zero. In the third step an adaptive observer-based method is carried out for the estimation of the side slip angle. The method also gives an estimation of the roll angles of the unsprung masses, which are important in the monitoring of the pitching dynamics.

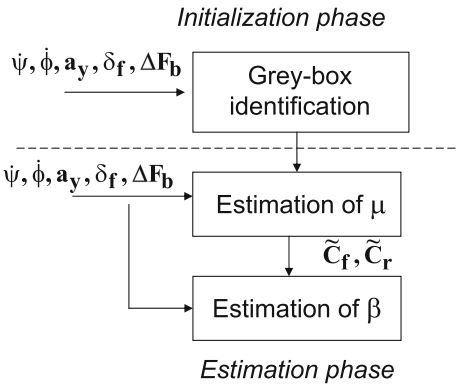


Fig. 2.16 The three-step estimation procedure

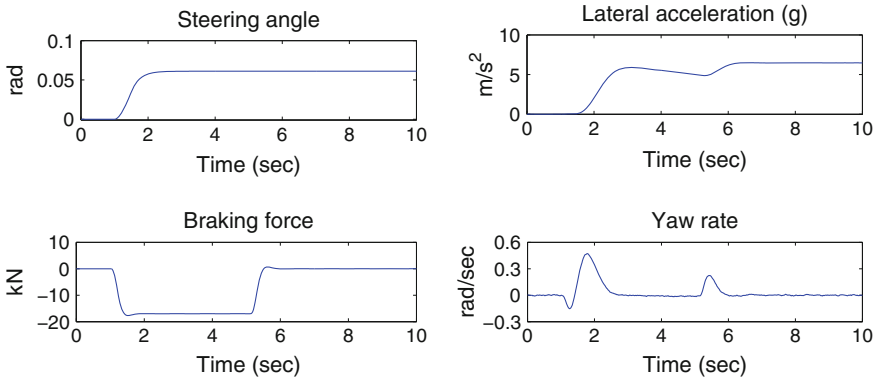


Fig. 2.17 Input and output signals in the identification step

Table 2.8 Result of the identification

Value	α_1	α_2	α_3	α_4
Actual	0.1174	26.6950	−0.0211	0.0266
Estimated	0.1116	26.6090	−0.0210	0.0266
Relative error	0.0491	0.0032	0.0048	0.0020
Value	I_{zz}	I_{xz}	μC_f	μC_r
Actual	34.9170	4.2	465.6	626.4
Estimated	34.9867	4.0062	465.0597	625.5661
Relative error	0.0020	0.0461	0.0012	0.0013

In what follows the three-step procedure is demonstrated through a simulation example. The preliminary estimation of the unknown parameters in the vehicle model is carried out in a vehicle manoeuvre in which the vehicle has started and already covered a certain distance. It is assumed that the manoeuvre has a short duration and the adhesion coefficient is constant. Using the measured signals the unknown parameters of the vehicle model are estimated. Obviously, when the model parameters are known, this step need not be performed.

Figure 2.17 presents the input and output signals of the simulation procedure, i.e., the steering angle, the lateral acceleration, the yaw rate and the difference between the brake forces. In the simulation example noise signals are added to the measured signals, which cause 2–3 % relative error. In the identification method it is assumed that the difference between the brake forces is available. Using the LS method four parameters are identified according to Eqs. (2.122) and (2.124) then the physical parameters are calculated. Table 2.8 shows the estimated values with their relative errors. In practice the difference between the brake forces is not always available. It is assumed, however, that if the brake forces are generated in a symmetrical way ΔF_b is approximately zero. In this case one of the estimated parameters must be known, e.g., the parameter I_{zz}.

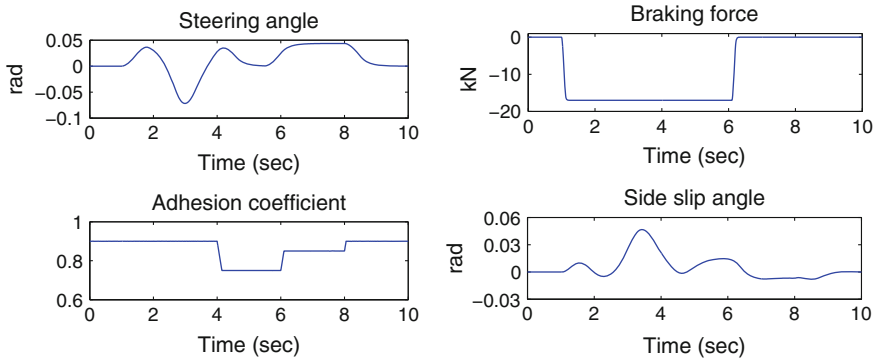


Fig. 2.18 Input and output signals in the estimation algorithm

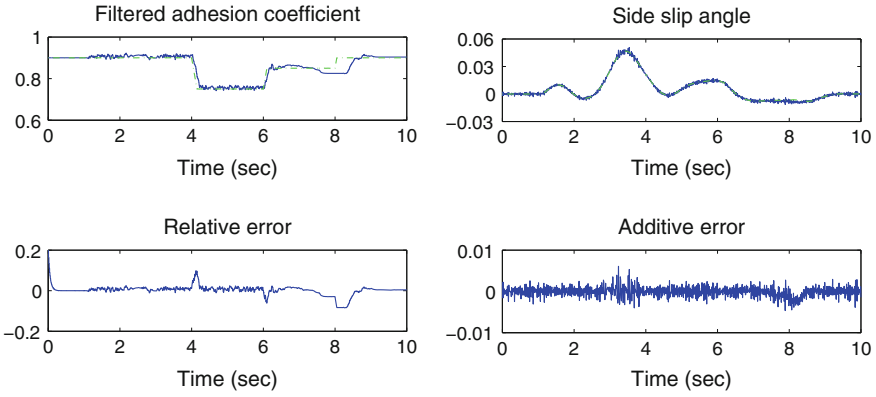
Then the estimation of the side slip angle and the adhesion coefficient are carried out. The signals in the simulation procedure are illustrated in Fig. 2.18. The measured signals are the steering angle, the yaw rate, the roll rate, the difference in the braking forces and the lateral acceleration. In Fig. 2.18 the side slip angle and the adhesion coefficient are also illustrated. These signals, however, are used for validation purposes, and they are assumed not to be available in the identification procedure. The identification procedure is performed in an on-line way, i.e., the identification of both the adhesion coefficient and the side slip angle is performed during the vehicle manoeuvres.

Then two identification steps are carried out: first, the adaptive method using a partial integration method for the adhesion coefficient, second, the adaptive observer-based method for the side slip angle. The result of the estimation of the side force coefficient approximates the vary of the real side force coefficient below an acceptable limit. In order to filter out the noises from the estimated signal a filtering procedure is also performed, which is illustrated together with its relative error in Fig. 2.19a. The result of the estimation of the side slip angle is illustrated in Fig. 2.19b. The estimation of the side force coefficient tends to the actual side force coefficient within a predefined acceptable limit.

2.7.3 Fault Estimation in LPV Systems

Any reconfiguration scheme rely on a suitable FDI component. There are a lot of approaches to design a detection filter, see, e.g., Chen and Patton (1999). The LPV setting, however, narrows the available tools.

In contrast to the LTI case in the LPV framework stability cannot be guaranteed in algebraic terms, e.g., by requiring that the "frozen" LTI systems are stable. Besides the technical difficulties of the potential design process this fact implies that algebraic methods of the classical LTI FDI filter design, see, e.g., Gertler (1998), Varga (2008), are not suitable for the LPV setting. In the LPV framework the only practical solution



(a) side force coefficient (b) side slip angle

Fig. 2.19 Estimated signals through simulation

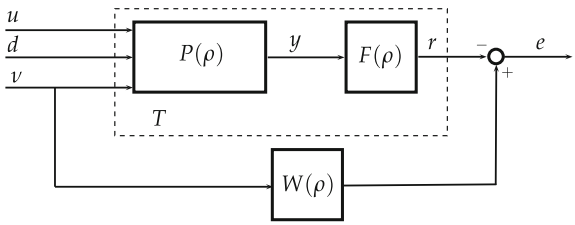


Fig. 2.20 Norm based detector design problem

is to require quadratic stability which can be cast as a set of LMI feasibility problems. The so called geometric approach of the FDI meets these requirements and often leads to successful detection filter design, for details see Balas et al. (2003), Bokor and Balas (2004), Edelmayer et al. (2004).

As a high level approach, the FDI filter design problem often can be cast in the model matching framework depicted on Fig. 2.20. The LPV paradigm permits to cast a nonlinear system as a linear time-varying (LTV) one, i.e., the residual can be expressed as

$$r = T_{ru}u + T_{rd}d + T_{rv}v. \tag{2.126}$$

Hence, to achieve robustness in the presence of disturbances and uncertainty, multi objective optimization-based FDI schemes can be proposed where an appropriately selected performance index has to be chosen to enhance sensitivity to the faults and simultaneously attenuate disturbances: the robust disturbance rejection condition is formulated as

$$\|T_{rd}\|_\infty = \sup_{\|v\|_2=1, \rho\in\mathscr{P}} \|r\|_2, \tag{2.127}$$

is to be minimized.

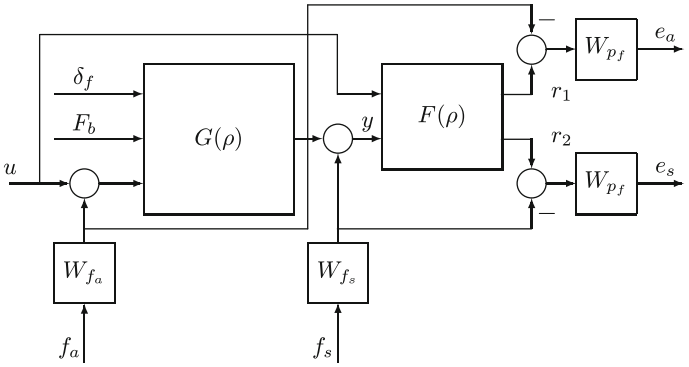


Fig. 2.21 Open loop interconnection structure for FDI filter design

This is a usual worst-case filtering problem and the corresponding design criteria can be formulated as a convex optimization problem by using LMIs. The main problem here is that the sensitivity and robustness conditions are conflicting. In the LTI framework it means that both sensitivity to faults and insensitivity to unknown inputs cannot be achieved at the same frequencies. Faults having similar frequency characteristics as those of disturbances might go undetected. While the design problem is non-convex, in general, Henry and Zolghadri (2004) proposes a scheme that can handle the problem by using LMI techniques.

A specific structure that fits the norm based approach, containing the weighted open-loop system, which includes the yaw–roll model $G(\rho)$ and the parameter-dependent FDI filter $F(\rho)$, and elements associated with performance objectives is depicted on Fig. 2.21. In the diagram, u is the control input, δ_f and F_b represent the disturbance signals, while y is the measured output. The FDI filter takes the measured outputs and the control inputs, thus, the effect of the control input is attenuated on residual outputs. In the figure, f_a is the actuator fault and f_s is the sensor fault. The e_a and e_s represents the weighted fault estimation errors associated with failures.

The weight W_{p_f} is the fault detection performance weight, which reflects the relative importance of the different frequency domains. The weighting function W_{p_f} chosen for fault estimation errors can be considered as penalty function, i.e., the weight should be large in the frequency range in which small errors are desired and small in which larger errors can be tolerated. The size of the frequency response of weight W_{p_f} should be large at low frequency to achieve the integral action for fault estimation. The weight W_{f_a} represents the size of possible fault in the actuator channel. The weight W_{f_s} takes sensor failure into consideration in the FDI filter design.

The augmented plant of the filtering problem has $w = \begin{bmatrix}\delta_f & F_b & f_a & f_s & u\end{bmatrix}^T$ as the disturbance input and $e = \begin{bmatrix}e_a & e_s\end{bmatrix}^T$ the performance output which are used to evaluate the estimation quality. The design requirement for $\mathscr{H}_\infty$ residual generation is to maximize the effect of the fault on the residual and simultaneously minimize the

effect of exogenous signals (δ_f, F_b, u) on the residual. Further details on the design can be found in Grenaille et al. (2008).

For illustrative purposes let us consider an FDI design for a suspension system, where possible faults of the actuators (loss of effectiveness) can be detected by reconstructing the actual suspension forces. Having measured the signals $y_1 = \dot{x}_3$, $y_2 = \dot{x}_4$ and $y_3 = x_2 - x_1$ an inversion based detection filter is designed.

Recall that the state space representation of the quarter-car model can be formalized with the state vector $x = \left[x_1\ x_2\ x_3\ x_4\right]^T$, where x_1 and x_2 denote the vertical displacement of the sprung mass and the unsprung mass, respectively, and x_3, x_4 denote their derivatives.

$$\dot{x}_3 = \frac{1}{m_s}(r_k(x_2 - x_1) + r_b(x_4 - x_3) + b_s^{nl}\rho_b\sqrt{\rho_b(x_4 - x_3)} - F), \tag{2.128}$$

$$\dot{x}_4 = \frac{1}{m_u}(-r_k(x_2 - x_1) - r_b(x_4 - x_3) - k_t(x_2 - d) - \\ - b_s^{nl}\rho_b\sqrt{\rho_b(x_4 - x_3)} + F), \tag{2.129}$$

where $r_b = b_s^l - b_s^{sym}\rho_b$ and $r_k = k_s^l + k_s^{nl}\rho_k$, while the chosen scheduling variables are $\rho_b = sgn(x_4 - x_3)$ and $\rho_k = (x_2 - x_1)^2$, respectively.

In the construction of the filter the first step is to express F from (2.128) and in these expression we plug in the known values y_i:

$$F = |z| + b_s^{nl}\rho_b\sqrt{|z|} + r_k y_3 - m_s y_1. \tag{2.130}$$

In this expression the value of the relative velocity z is not measured. The road disturbance is an unknown input signal but from the Eqs. (2.128) and (2.129) one has

$$m_s\dot{x}_3 + m_u\dot{x}_4 = -k_t(x_2 - d). \tag{2.131}$$

By plugging back the obtained expressions in the original equations one has the system $\dot{x}_3 = \frac{r_k}{m_s}(x_2 - x_1) - \frac{r_k}{m_s}y_3 + y_1$ and $\dot{x}_4 = -\frac{r_k}{m_u}(x_2 - x_1) + \frac{r_k}{m_u}y_3 + y_2$, where the relative velocity is not measured. The resulting LPV system

$$\dot{z} = -r_k m_e z + r_k m_e y_3 + y_2 - y_1, \tag{2.132}$$

with $m_e = \frac{m_u + m_s}{m_u m_s}$ will be observable.

For a semi-active actuator one can compare the value of the reconstructed force with the nominal value of the damper force given for the specific value of the damper velocity by the characteristics. If these two values differ considerably, a fault event must be signaled. For active actuators however, since the real actuators might present a saturation effect, it is necessary to check in addition, if the actual forces are lower then those corresponding to the saturation level of the actuators, i.e., it is not enough to compare the reconstructed forces with the force demands provided by the robust LPV controllers.

To obtain the final fault detection filter the equations of the actuator dynamics are used as:

$$\dot{\tilde{x}}_5 = -\beta\tilde{x}_5 + \alpha A_P\hat{z} + \gamma Q_{0,nom}(\hat{F})\tilde{x}_6, \tag{2.133}$$

$$\dot{\tilde{x}}_6 = -\frac{1}{\tau_{nom}}\tilde{x}_6 + \frac{1}{\tau_{nom}}u_a, \tag{2.134}$$

where $\hat{z}$ and $\hat{F}$ are the estimated damper velocity and damper force values, respectively. A possible actuator fault affects the terms Q_0 through a modified value of P_s and the time constant τ, respectively. The nominal values of these parameters (i.e., for the fault free case) are denoted by the subscript nom.

For the fault free case one should have $e_5 = x_5 - \tilde{x}_5 \approx 0$ and $e_6 = x_6 - \tilde{x}_6 \approx 0$, respectively. If $e = \|e_5\|_2 + \|e_6\|_2$ is greater than a given threshold, then a fault must be present in the system and a fault signal is emitted to the higher level controller, used in the controller reconfiguration process. Since the initial conditions are not known, an (LPV) observer need to be constructed for (2.132) and (2.133), (2.134) respectively. For a LPV system that depends affinely on the scheduling variables an LPV observer can be designed using LMI techniques: let us recall that an LPV system is said to be quadratically stable if there exist a matrix $P = P^T > 0$ such that $A(\rho)^T P + PA(\rho) < 0$ for all the parameters ρ. A necessary and sufficient condition for a system to be quadratically stable is that this condition holds for all the corner points of the parameter space, i.e., one can obtain a finite system of linear matrix inequalities (LMIs) that have to be fulfilled for $A(\rho)$ with a suitable positive definite matrix P.

In order to obtain a quadratically stable observer the LMI

$$A_o^T(\rho)P + PA_o(\rho) < 0 \tag{2.135}$$

must hold for suitable $K(\rho)$ and $P = P^T > 0$, with $A_o = A + KC$. By introducing the auxiliary variable $L(\rho) = PK(\rho)$, one has to solve the following set of LMIs on the corner points of the parameter space:

$$A(\rho)^T P + PA(\rho) - C^T L(\rho)^T - L(\rho)C < 0. \tag{2.136}$$

By solving these LMIs a suitable observer gain is obtained:

$$K(\rho) = P^{-1}L(\rho). \tag{2.137}$$

In the simulation example result the reconstructed force is illustrated by the solid blue line in the upper part of Fig. 2.22.

The force is compared with the force produced by a fault free suspension system (dashed line). The FDI filter gives the signals depicted in blue in the bottom part of Fig. 2.22, while the red signal is the chosen threshold level expressed in a given

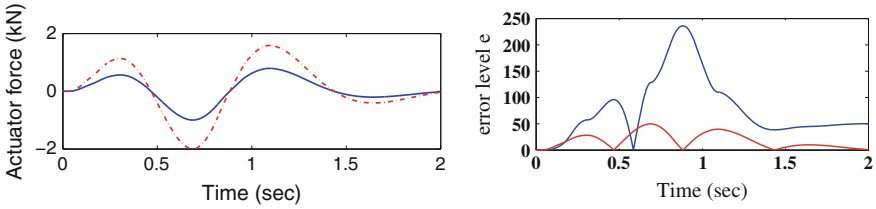


Fig. 2.22 The result of the FDI procedure

percent of the desired force. Since the obtained error level will be greater than this threshold, a fault signal is emitted indicating a faulty actuator.

The threshold level influences the fault-detection delay, i.e., high threshold level corresponds to increased delay. However, due to disturbances, sensor noises and the modeling uncertainties this level cannot be arbitrarily small and it is determined using engineering knowledge.

http://www.springer.com/978-3-319-46124-3

Robust Control Design for Active Driver Assistance Systems
A Linear-Parameter-Varying Approach
Gaspar, P.; Szabo, Z.; Bokor, J.; Nemeth, B.
2017, XIII, 293 p. 107 illus., 48 illus. in color., Hardcover
ISBN: 978-3-319-46124-3